study established the concept of using BM-MNCs for therapeutic angiogenesis, limited information is available about the long-term safety and efficacy of this strategy.

The purpose of the present study was to determine the long-term safety and clinical impact of BM-MNC transplantation for "no-option" patients with thromboangiitis obliterans.

Methods

Patients

Eight patients with thromboangiitis obliterans were treated with an autologous transplantation of BM-MNCs between March 2002 and September 2004. The diagnosis of thromboangiitis obliterans was based on the criteria proposed by Olin[12]: (1) onset before age 45; (2) current (recent) history of tobacco use; (3) the presence of distal-extremity ischemia (infrapopliteal or infrabrachial) indicated by claudication, rest pain, ischemic ulcers, or gangrene; (4) exclusion of autoimmune or connective tissue diseases, hypercoagulable states, and diabetes mellitus; (5) exclusion of a proximal source of emboli by echocardiography and arteriography; and (6) consistent arteriographic findings in the clinically involved and noninvolved limbs.

Patients qualified for cell transplantation if they had chronic limb ischemia, with rest pain or a nonhealing ischemic ulcer, present for a minimum of 4 weeks without evidence of improvement in response to conventional drug therapy; showed angiographic evidence of vasculopenia in the affected limb; and were not candidates for percutaneous or surgical revascularization. The exclusion criteria included severe concurrent illness, the presence of proliferative diabetic retinopathy, and a history or clinical evidence of a malignant disorder.

All the patients involved in the present study received continuous medical therapy for >2 months before BM-MNC transplantation to confirm that conventional measures would be insufficient to achieve improvement in rest pain or skin ulcer/gangrene. During this period, no surgical therapies such as bypass grafting, extensive debridement, skin grafting, or limb amputation were performed. In addition, the patients were admitted to the hospital for a minimum of 1 month before BM-MNC transplantation to exclude the likelihood of spontaneous improvement in ischemic symptoms resulting from an enrollment bias. It should be also pointed out that the patients remained in the hospital and received the same therapy for at least 1 month after BM-MNC transplantation to avoid changes in their treatment.

BM-MNC Transplantation

While the patients were under general anesthesia, marrow cells were aspirated from the ileum. BM-MNCs were sorted on an AS-104 blood-cell separator (Fresenius HemoCare, Redmond, Wash) and concentrated to a final volume of ≈50 mL. After bone marrow cells were sorted on the AS-104 blood-cell separator, a small fraction of the cells was used for BM-MNC counting; the concentration of BM-MNCs in the final product was determined by using a microscope counting chamber after May-Giemsa staining. By using another fraction of cells, the number of $CD34^+$ cells in the BM-MNCs was also determined by fluorescence-activated cell sorting (FACS SCAN flow cytometer; Becton Dickinson, San Jose, Calif). The cells were incubated with the FITC-conjugated mouse monoclonal antibody against human CD34 (clone 581; Becton Dickinson) according to manufacturer's instructions.

For each patient, ≈100 aliquots of BM-MNCs (0.5 mL per aliquot) were administered via a syringe with a 27-gauge needle. Injection was performed into 9 lower limbs in 7 of the patients and the bilateral hands in 1. Injection sites were arbitrarily selected according to angiographic findings (ie, the degree of vasculopenia) and included calf muscles such as the soleus and gastrocunemius muscles as well as the sole muscles of the foot. For the patient with hand ischemia, injection was performed in palm muscles.

Assessment of Short-Term Outcome

Ischemic pain was assessed with a visual analog pain scale (VAS) with 10 levels. Ischemic ulcers were documented by color photography. Resting ankle-brachial pressure index (ABI) was calculated as the quotient of absolute ankle pressure and brachial pressure (the patient who received BM-MNC transplantation in his hands was excluded from ABI analysis). Angiographic assessment was performed with magnetic resonance angiography, computed tomographic angiography, or digital subtraction angiography. Adverse events were defined as death, limb amputation, pathological angiogenesis, recurrence/worsening of ischemic symptoms (ie, rest pain, skin ulcer, gangrene), myocardial infarction, stroke, and malignant disease.

Assessment of Long-Term Outcome

The mean length of follow-up was 684±549 days (range 103 to 1466). Patients were followed up by history analysis, physical examination, routine blood testing, ABI, and angiography at prescribed intervals during the first year, after which they were contacted at an outpatient clinic or by telephone to track events.

Data Analysis

All data are presented as mean±SD (range) or frequencies (percentage).

The authors had full access to and take full responsibility for the integrity of the data. All authors have read and agree to the manuscript as written.

Results

Diagnosis

The diagnosis of thromboangiitis obliterans was made according to the criteria described above. Among the 8 patients, only patient 6 did not completely fulfill the criteria; ie, this patient had no history of tobacco use (Table 1). Laboratory screening excluded the possibility of other underlying diseases, however, including autoimmune and connective tissue diseases. It should be also pointed out that patient 6 had diabetes mellitus at the time of cell transplantation but not at the onset of thromboangiitis obliterans. With the typical characteristic angiographic findings of thromboangiitis obliterans, such as multiple segmental arterial involvement (skip lesions) and "cork-screw" collateral vessels, we diagnosed patient 6 as having thromboangiitis obliterans, even though the patient did not have a history of tobacco use.

Patient Characteristics

The demographic and clinical data of the 8 patients are shown in Table 1. The mean age of the patients enrolled was 46±14 years (range 28 to 63). Seven patients (88%) were male. One patient had undergone prior femoral-tibial artery bypass grafting, and 1 had undergone sympathetic ganglion block. These treatments were performed >1 year before BM-MNC transplantation. Seven patients (88%) had a history of smoking, all of whom stopped smoking at least 1 month before transplantation.

Short-Term Outcome

The total volume of cells aspirated from the ileum was 728±72 mL (range 600 to 800) per patient, and the total volume of injected BM-MNCs was 45±7 mL (range 30 to 50) per patient. Total number of injected BM-MNCs was $3.5\pm0.8\times10^9$ (range 2.0 to 4.7×10^9), and that of $CD34^+$ cells was $6.8\pm2.6\times10^7$ (range 2.4 to 9.7×10^7).

TABLE 1. Patient Characteristics

Patient	Age	Sex	Fontaine Stage	Previous Treatment	DM	HT	HLP	Smoking	BM-MNC ($\times 10^9$)	$CD34^+$ in BM-MNC ($\times 10^7$)	ABI, Baseline	ABI, 1 Month	VAS, Baseline	VAS, 1 Month
1	63	M	III(lt)	Bypass graft	−	−	+	+	3.0	6.6	0.34	0.55	5	0
2	31	M	IV(rt)	Medical	−	−	−	+	4.7	9.7	0.49	0.39	5	1
3	52	M	IV(lt)	Medical	−	−	−	+	4.1	9.0	0.65	0.67	7	2
4	28	M	IV(lt)	Sympathetic ganglion block	−	−	−	+	2.0	6.8	0.50	0.26	5	0
5	32	M	IV(rt)	Medical	−	−	−	+	3.8	2.4	−	−	5	2
			IV(lt)								−	−	5	2
6	55	F	IV(lt)	Medical	+	+	−	−	3.4	4.0	0.53	0.51	4	3
7	63	M	III(rt)	Medical	−	+	−	+	3.0	9.1	1.10	0.91	5	3
			IV(lt)								0.76	0.94	5	3
8	43	M	IV(rt)	Medical	−	+	−	+	3.6	6.8	1.00	1.04	5	0
			III(lt)								1.00	1.07	5	0

DM indicates diabetes mellitus; HT, hypertension; and HLP, hyperlipidemia.

Angiographic assessment at 4 weeks after transplantation revealed an apparent increase in limb vascularity in 3 of the 8 (38%) patients (4 of the 11 limbs) (Figure 1). Hemodynamic assessment also failed to document evidence of improved collateral development. Specifically, an increase in ABI (>0.1) was observed in 2 of 7 (29%) patients (2 of 8 limbs), whereas a decrease in ABI (>0.1) was observed in 2 of 7 (29%) patients (2 of 8 limbs). As a result, mean ABI measured at 4 weeks (0.71±0.30) did not differ from that at the baseline (0.70±0.27). Because 2 patients had sites of arterial occlusion distal to the ankle, they showed normal ABIs before treatment. Even after the exclusion of these 2 patients, ABI showed no changes between before (0.55±0.15) and after transplantation (0.55±0.24).

In contrast to the angiographic and hemodynamic results, improvement in limb status was observed in all 8 patients (100%). Improvement in VAS was observed in all 11 limbs, with a decrease from a mean of 5.1±0.7 to 1.5±1.3. Furthermore, complete pain relief was achieved in 4 of the 11 limbs (36%). Improvement in skin ulcers was also observed in all 8 limbs (100%), with complete healing in 7 (88%). Although surgical amputations of the distal limb were performed in 2 patients at 1 month, these operations were intentionally scheduled to be performed after transplantation with the expectation of sufficiently improving the limb perfusion to distally advance the site of amputation (Table 2; Figure 2A and 2B).

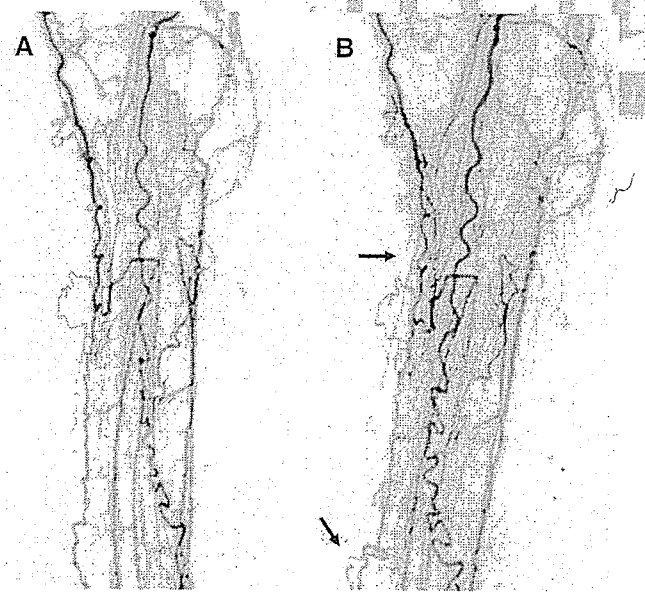

Figure 1. Digital subtraction angiography at (A) baseline and (B) 1 month after cell transplantation. Arrows indicate newly visible collateral vessels at the calf level.

Long-Term Outcome

The mean follow-up period was 684±549 days (range 103 to 1466). At the final follow-up, VAS score remained unchanged from that observed at 1 month after transplantation in 5 of the 8 patients (63%). The mean VAS score at follow-up also remained low (2.3±1.9) compared with that observed at baseline (5.1±0.7).

In contrast to the pain scale results, adverse events were observed in as many as 4 patients (50%) (Table 2). At age 30

TABLE 2. Adverse Outcomes After Autologous Transplantation of BM-MNCs in Patients With Thromboangiitis Obliterans

Adverse Outcomes	30 Days	Final Follow-Up
Death	0	1 (13)
Major amputation	0	0
Minor amputation	2 (25)*	0
Unexpected angiogenesis	0	1 (13)
Recurrence/worsening of skin ulcer/gangrene	0	2 (25)†
Recurrence/worsening of pain	0	1 (13)
Cardiovascular event	0	0
Cerebrovascular event	0	0
Malignancy	0	0

Values are expressed as n (%).

*Amputation was intentionally scheduled to be performed at 1 month after transplantation.

†One patient was the same one who developed unexpected angiogenesis.

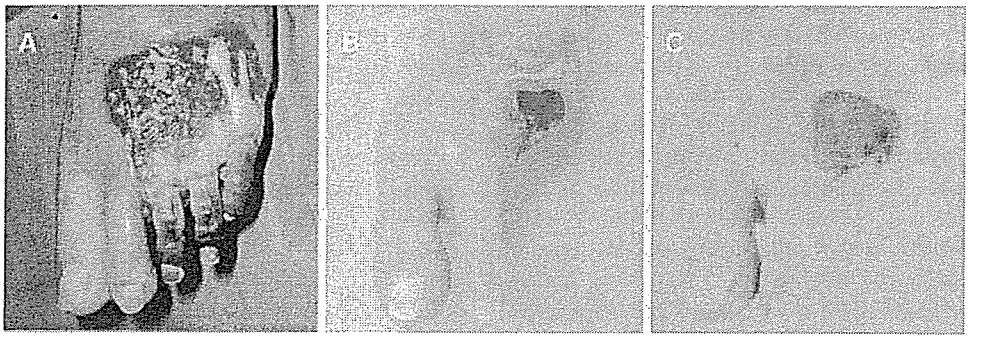

Figure 2. Skin ulcer at (A) 1 month, (B) 2 months, and (C) 4 months after cell transplantation. The patient had far-advanced gangrene, and total limb integrity could not be fully preserved. The patient received a prescheduled amputation of the distal limb at 1 month, and the skin ulcer continued to improve thereafter. At 4 months, however, the skin lesion began to enlarge.

years, patient 4 suddenly died of an unknown cause at 20 months after transplantation. This patient had previously been a smoker, but had stopped smoking before cell transplantation. He had no history of diabetes, hypertension, or hyperlipidemia. Furthermore, ^{201}thallium myocardial scan performed before BM-MNC transplantation showed no signs of myocardial ischemia. After cell transplantation, his limb pain disappeared within 1 week and his skin ulcer resolved by 1 month. Thereafter, he was completely free of limb symptoms. Twenty months after cell transplantation, however, he was found dead at his home. He had never experienced chest pain up to the time of his death. Because no autopsy was performed, the cause of his death remains unknown.

Patient 6 showed worsening of an ischemic ulcer at 4 months. The patient had far-advanced gangrene, and total limb integrity could not be fully preserved. The patient underwent a prescheduled amputation of the distal limb at 1 month (see Short-Term Outcome) (Figure 2A), and the skin ulcer continued to improve thereafter (Figure 2B). At 4 months, however, the skin lesion began to increase in size (Figure 2C). The patient subsequently received a second round of cell therapy.

In patient 7, despite complete healing of the skin ulcer, rest pain did not completely resolve after transplantation, with a VAS score of 3 at 1 month. At 8 months, the patient experienced worsening of rest pain (VAS score=4). After a combination of exercise training and maximal drug therapy, the pain improved and became well tolerated.

Patient 8 experienced swelling and recurrence of the skin ulcer in his foot at 7 months. Computed tomographic angiography documented an early venous return of contrast material in his right limb (Figure 3B) that was not observed at the baseline (Figure 3A). Ultrasound examination disclosed an arterialized waveform in the dorsal vein at the base of his third toe, suggesting the presence of an arteriovenous shunt. By 1 year, the swelling and skin ulcer had spontaneously regressed. The systolic pulsatile component in the venous waveform was found to be diminished on ultrasound examination, and early venous filling had disappeared on computed tomographic angiography (Figure 3C).

Discussion

In the present unblinded and uncontrolled pilot study, we documented that the transplantation of BM-MNCs was associated with an improvement in ischemic symptoms for up to 4 years. Indeed, VAS scores improved from 5.1±0.7 to 2.3±1.9 at follow-up. Furthermore, skin ulcers remained completely healed in 6 of 7 patients. In this regard, the present findings extend previous observations[11] by establishing the potential long-term benefit of BM-MNC transplantation for the treatment of arterial insufficiency.

It should be noted, however, that half of the patients suffered adverse events during follow-up. Such a high rate of adverse events cannot be explained by the natural course of the disease itself. In general, the prognosis of patients with thromboangiitis obliterans is directly related to tobacco

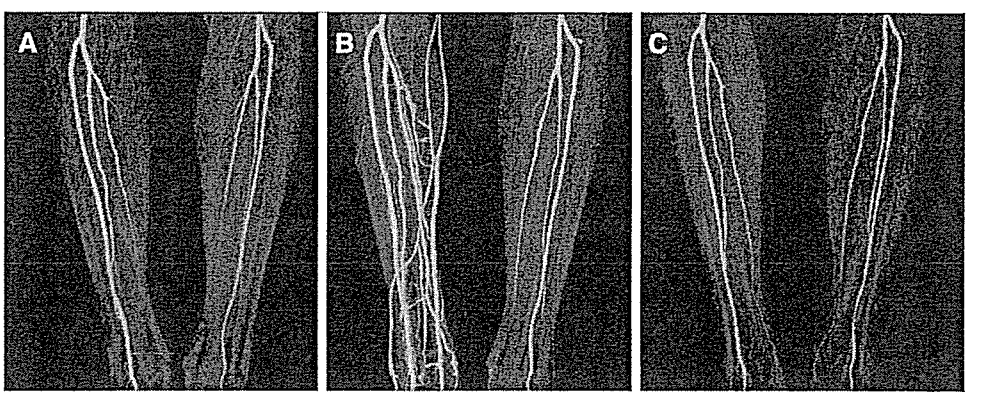

Figure 3. Computed tomographic angiography at (A) baseline, (B) 7 months, and (C) 1 year after cell transplantation. Early venous return of contrast material observed at 7 months spontaneously regressed by 1 year.

use.[12,13] Patients who are able to stop smoking avoid the recurrence of the disease and amputation.[14] In addition, unlike those with atherosclerosis of the extremities, these patients rarely show involvement of visceral vessels and do not appear to be at an increased risk of stroke or myocardial infarction. The mortality rates are thus not higher than those of age- and sex-matched populations.[15,16] It is entirely possible that the high rate of adverse events observed in our patients may have been directly related to BM-MNC transplantation rather than to the progression of the disease itself.

Patient 4 suddenly died at 20 months after transplantation at the age of 30 years. The deaths of patients receiving BM-MNC transplantation were previously reported in the TACT study, in which 2 of 25 patients died of acute myocardial infarction within 24 weeks after transplantation.[11] The patients' backgrounds in the TACT study, in terms of age and comorbidity, may have been totally different from those of our study, in which only patients with thromboangiitis obliterans were recruited. As mentioned above, in patients with thromboangiitis obliterans, coronary involvement is rare, and they usually do very well as long as they discontinue smoking.[12–16] Patient 4 had no risk factors for atherosclerosis and stopped smoking before BM-MNC transplantation. Furthermore, ^{201}thallium scintigraphy performed before transplantation documented no sign of myocardial ischemia. Considering the patient's background and the natural course of the disease,[12–16] the possibility that his death was related to BM-MNC transplantation cannot be excluded. In this regard, several studies have suggested the possible role of BM-MNCs in atherogenesis. A recent report by Silvestre et al,[17] for example, demonstrated that the transplantation of BM-MNCs into ischemic limbs of apolipoprotein E–knockout mice led to a significant increase in atherosclerotic plaque size at a distant site. More recently, George et al[18] have also shown that an intravenous injection of bone marrow cells into apolipoprotein E–knockout mice results in an increase in atherosclerotic lesion size, whereas an injection of endothelial progenitor cells influences plaque stability. These reports indicate that attempts to enhance neovascularization by using BM-MNCs could also enhance unwanted plaque growth and instability, thus suggesting the possibility that our young patient died of an acute coronary event due to accelerated atherogenesis after BM-MNC transplantation.

We also encountered the development of an arteriovenous shunt, which could be a potential consequence of BM-MNC transplantation. Indeed, concerns have been raised about the potential adverse effects of cell transplantation, ie, unregulated differentiation and proliferation. Wakitani et al[19] reported that teratoma formation could occur after embryonic stem cell transplantation. Yoon et al[20] documented intramyocardial calcification after the transplantation of bone marrow cells in rats. Our observations may provide another cautionary example of unregulated differentiation and proliferation. Although the arteriovenous shunt in our case was self-limited, it may represent unwanted angiogenesis; thus, careful monitoring is warranted for future patients who receive BM-MNC transplantation.

Worsening or recurrence of ischemic symptoms was observed in 3 patients. The short-term outcome at 1 month was poor in these patients except in the patient with an arteriovenous shunt. The improvement in rest pain was not substantial in 1 patient. Healing of the skin ulcer was incomplete in another. It is anticipated that a poor response 1 month after BM-MNC transplantation could result in a poor long-term outcome. It is important to note that, in the latter patient with incomplete healing of the skin ulcer, the angiographic improvement of the collateral network at 1 month remained unchanged at 5 months when worsening of the skin ulcer was observed. It is suggested that the temporal sequence of improvement in ischemic limb status does not necessarily parallel the temporal evolution of collateral development.

Conclusions

In this unblinded and uncontrolled pilot study, long-term adverse events after BM-MNC transplantation, including death and unfavorable angiogenesis, were observed in half of the patients with thromboangiitis obliterans. Given the current incomplete knowledge of the safety and efficacy of this strategy, careful long-term monitoring is required for future patients receiving BM-MNC transplantation.

Sources of Funding

This work was supported by Health and Labor Sciences Research Grants (H16-009, H16-017, H17-009), by Ministry of Health, Labor and Welfare Research Grants for Cardiovascular Disease (16C-6, 18C-4), and by grants from the New Energy and Industrial Technology Development Organization and the Japan Cardiovascular Research Foundation.

Disclosures

None.

References

1. Belch JJ, Topol EJ, Agnelli G. Critical issues in peripheral arterial disease detection and management: a call to action. *Arch Intern Med.* 2003;28: 884–892.
2. Dormandy JA, Rutherford RB. Management of peripheral artery disease (PAD). TASC Working Group. TransAtlantic InterSociety Consensus (TASC). *J Vasc Surg.* 2000;31:S1–S296.
3. Isner JM, Rosenfield K. Redefining the treatment of peripheral artery disease. *Circulation.* 1993;88:1534–1557.
4. Takeshita S, Zheng LP, Brogi E, Kearney M, Pu LQ, Bunting S, Ferrara N, Symes JF, Isner JM. Therapeutic angiogenesis: a single intraarterial bolus of vascular endothelial growth factor augments revascularization in a rabbit ischemic hind limb model. *J Clin Invest.* 1994;93:662–670.
5. Isner J, Asahara T. Angiogenesis and vasculogenesis as therapeutic strategies for postnatal neovascularization. *J Clin Invest.* 1999;103: 1231–1236.
6. Asahara T, Murohara T, Sullivan A, Silver M, van der Zee R, Li T, Witzenbichler B, Schatteman G, Isner JM. Isolation of putative progenitor cells for angiogenesis. *Science.* 1997;275:964–967.
7. Asahara T, Masuda H, Takahashi T, Kalka C, Pastore C, Silver M, Kearney M, Magner M, Isner JM. Bone marrow origin of endothelial progenitor cells responsible for postnatal vasculogenesis in physiological and pathological neovascularization. *Circ Res.* 1999;85:221–228.
8. Shi Q, Rafii S, Wu M. Evidence for circulating bone marrow–derived endothelial cells. *Blood.* 1998;92:362–367.
9. Kalka C, Masuda H, Takahashi T, Kalka-Moll WM, Silver M, Kearney M, Li T, Isner JM, Asahara T. Transplantation of ex vivo expanded endothelial progenitor cells for therapeutic neovascularization. *Proc Natl Acad Sci U S A.* 2000;97:3423–3427.
10. Shintani S, Murohara T, Ikeda H, Ueno T, Sasaki K, Duan J, Imaizumi T. Augmentation of postnatal neovascularization with autologous bone marrow transplantation. *Circulation.* 2001;103:897–903.
11. Tateishi-Yuyama E, Matsubara H, Murohara T, Ikeda U, Shintani S, Masaki H, Amano K, Kishimoto Y, Yoshimoto K, Akashi H, Shimada K,

Iwasaka T, Imaizumi T. Therapeutic angiogenesis for patients with limb ischemia by autologous transplantation of bone marrow cells: a pilot study and a randomized controlled trial. *Lancet.* 2002;360:427–435.
12. Olin JW. Thromboangiitis obliterans (Buerger's disease). *N Engl J Med.* 2000;343:864–869.
13. Olin JW, Young JR, Graor RA, Ruschhaupt WF, Bartholomew JR. The changing clinical spectrum of thromboangiitis obliterans (Buerger's disease). *Circulation.* 1990;82(5 Suppl):IV3–IV8.
14. Matsushita M, Shionoya S, Matsumoto T. Urinary cotinine measurement in patients with Buerger's diseases: effects of active and passive smoking on the disease process. *J Vasc Surg.* 1991;14:53–58.
15. Szuba A, Cooke JP. Thromboangiitis obliterans: an update on Buerger's disease. *West J Med.* 1998;168:225–260.
16. Mills JL, Taylor LMJ, Porter JM. Buerger's disease in the modern era. *Am J Surg.* 1987;154:123–129.
17. Silvestre J-S, Gojova A, Brun V, Potteaux S, Esposito B, Duriez M, Clergue M, Le Ricousse-Roussanne S, Barateau V, Merval R, Groux H, Tobelem G, Levy B, Tedgui A, Mallat Z. Transplantation of bone marrow–derived mononuclear cells in ischemic apolipoprotein E–knockout mice accelerates atherosclerosis without altering plaque composition. *Circulation.* 2003;108:2839–2842.
18. George J, Afek A, Abashidze A, Shmilovich H, Deutsch V, Kopolovich J, Miller H, Keren G. Transfer of endothelial progenitor and bone marrow cells influences atherosclerotic plaque size and composition in apolipoprotein E knockout mice. *Arterioscler Thromb Vasc Biol.* 2005;25:2636–2641.
19. Wakitani S, Takaoka K, Hattori T, Miyazawa N, Iwanaga T, Takeda S, Watanabe TK, Tanigami A. Embryonic stem cells injected into the mouse knee joint form teratomas and subsequently destroy the joint. *Rheumatology (Oxford).* 2003;42:162–165.
20. Yoon Y, Park J, Tkebuchava T, Luedeman C, Losordo D. Unexpected severe calcification after transplantation of bone marrow cells in acute myocardial infarction. *Circulation.* 2004;109:3154–3157.

CLINICAL PERSPECTIVE

The favorable short-term outcome of bone marrow mononuclear cell transplantation (BM-MNC) transplantation has been established in patients with critical limb ischemia. However, the long-term outcome of this treatment strategy has not been determined yet. In our case series, we documented that long-term adverse events, including death and unfavorable angiogenesis, were observed in 4 of 8 patients receiving BM-MNC transplantation. The first patient suffered sudden death at 20 months after transplantation at 30 years of age. The second patient with incomplete healing of a skin ulcer showed worsening of the lesion at 4 months. The third patient had worsening of rest pain at 8 months. The last patient developed an arteriovenous shunt in the foot at 7 months, which spontaneously regressed by 1 year. Given the current incomplete knowledge on the safety and efficacy of this strategy, it is suggested that careful long-term monitoring is required in patients receiving BM-MNC transplantation. To our knowledge, this is the first report on the long-term outcome of transplantation of BM-MNCs for critical limb ischemia, and the first that documents the development of unfavorable angiogenesis and sudden death after therapeutic angiogenesis.

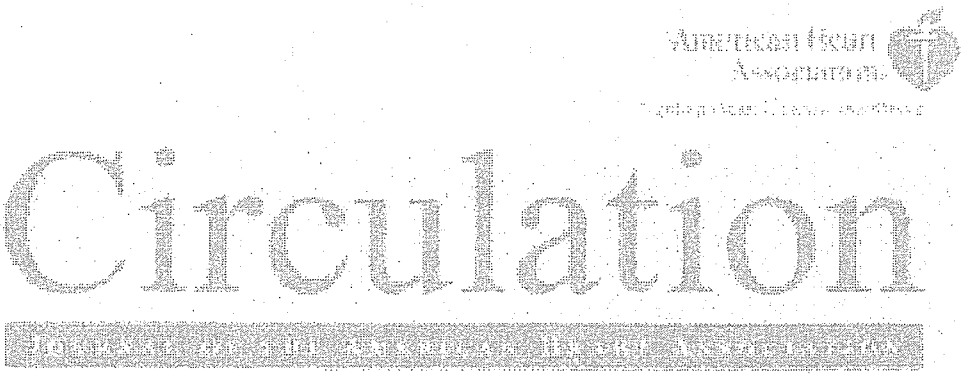

Am J Physiol Lung Cell Mol Physiol 290: L59–L65, 2006.
First published September 9, 2005; doi:10.1152/ajplung.00042.2005.

Prostacyclin agonist with thromboxane synthase inhibitory activity (ONO-1301) attenuates bleomycin-induced pulmonary fibrosis in mice

Shinsuke Murakami,[1,2] Noritoshi Nagaya,[1,3] Takefumi Itoh,[2] Masaharu Kataoka,[1] Takashi Iwase,[1] Takeshi Horio,[3] Yoshinori Miyahara,[4] Yoshiki Sakai,[5] Kenji Kangawa,[6] and Hiroshi Kimura[2]

[1]Department of Regenerative Medicine and Tissue Engineering, National Cardiovascular Center Research Institute, Osaka; [2]Second Department of Internal Medicine, Nara Medical University, Nara; [3]Department of Internal Medicine, National Cardiovascular Center, Osaka; [4]Department of Cardiac Physiology, National Cardiovascular Center Research Institute, Osaka; [5]Ono Pharmaceutical Co., Ltd. Research Headquarters, Osaka; and [6]Department of Biochemistry, National Cardiovascular Center Research Institute, Osaka, Japan

Submitted 20 January 2005; accepted in final form 1 September 2005

Murakami, Shinsuke, Noritoshi Nagaya, Takefumi Itoh, Masaharu Kataoka, Takashi Iwase, Takeshi Horio, Yoshinori Miyahara, Yoshiki Sakai, Kenji Kangawa, and Hiroshi Kimura. Prostacyclin agonist with thromboxane synthase inhibitory activity (ONO-1301) attenuates bleomycin-induced pulmonary fibrosis in mice. *Am J Physiol Lung Cell Mol Physiol* 290: L59–L65, 2006. First published September 9, 2005; doi:10.1152/ajplung.00042.2005.—The balance between prostacyclin and thromboxane A_2 (TXA_2) plays an important role in pulmonary homeostasis. However, little information is available regarding the therapeutic potency of these prostanoids for pulmonary fibrosis. We have recently developed ONO-1301, a novel long-acting prostacyclin agonist with thromboxane synthase inhibitory activity. Thus we investigated whether repeated administration of ONO-1301 attenuates bleomycin-induced pulmonary fibrosis in mice. After intratracheal injection of bleomycin or saline, mice were randomized to receive repeated subcutaneous administration of ONO-1301 or vehicle. Bronchoalveolar lavage (BAL) and histological analyses were performed at 3, 7, and 14 days after bleomycin injection. In vitro studies using mouse lung fibroblasts were also performed. ONO-1301 significantly attenuated the development of bleomycin-induced pulmonary fibrosis, as indicated by significant decreases in Ashcroft score and lung hydroxyproline content. ONO-1301 significantly reduced total cell count, neutrophil count, and total protein level in BAL fluid in association with a marked reduction of TXB_2. A single administration of ONO-1301 significantly increased plasma cAMP level for >2 h. In vitro, ONO-1301 and a cAMP analog dose-dependently reduced cell proliferation in mouse lung fibroblasts. The reduction in cell proliferation by ONO-1301 was attenuated by a protein kinase A (PKA) inhibitor. Furthermore, bleomycin mice treated with ONO-1301 had a significantly higher survival rate than those given vehicle. These results suggest that repeated administration of ONO-1301 attenuates the development of bleomycin-induced pulmonary fibrosis and improves survival in bleomycin mice, at least in part by inhibition of TXA_2 synthesis and activation of the cAMP/PKA pathway.

adenosine 3′,5′-cyclic monophosphate; fibroblast; neutrophil; survival

IDIOPATHIC PULMONARY FIBROSIS (IPF) is a life-threatening disease characterized by progressive dyspnea and worsening of pulmonary function (6, 22). The pathological features of IPF are fibroblast proliferation with increased amounts of extracellular matrix and varying degrees of persistent inflammation of the alveolar septa (22). Thus a novel therapeutic strategy against these abnormalities may be effective for the treatment of IPF.

Prostanoids, which are metabolites of arachidonic acid, are important regulators of pulmonary homeostasis. Prostacyclin inhibits migration, proliferation, and collagen synthesis in fibroblasts (14, 29). Conversely, thromboxane A_2 (TXA_2) promotes fibroblast proliferation, increases pulmonary vascular permeability, and induces lung inflammation (18, 21, 24). Interestingly, a recent study has demonstrated that the decreased ratio of prostacyclin synthesis to thromboxane synthesis is associated with the development of pulmonary fibrosis (4). Thus we hypothesized that compounds that regulate the balance between prostacyclin and TXA_2 may have beneficial effects in IPF.

Recently, we have developed a novel nonprostanoid long-acting prostacyclin agonist possessing a potent inhibitory activity against thromboxane synthase, named ONO-1301. Unlike prostacyclin, ONO-1301 does not possess a five-membered ring and allylic alcohol in its molecule, which contributes to the biological and chemical stability of this compound. As a result, this compound can be given by subcutaneous administration twice a day. Its inhibitory effect on thromboxane synthesis is mediated by binding of thromboxane synthase to 3-pyridine moiety and a carboxylic acid group in ONO-1301 (30).

Thus the purpose of this study was to investigate whether modulation of prostacyclin/TXA_2 balance by ONO-1301 attenuates bleomycin-induced pulmonary fibrosis and improves survival in bleomycin-injected mice.

METHODS

Animals. We used specific pathogen-free female C57BL/6 mice weighing 18–20 g. The mice were randomly given intratracheal injection of either bleomycin (Nippon Kayaku, Tokyo, Japan) or saline, and assigned to receive repeated administration of ONO-1301 or vehicle. This protocol resulted in the creation of three groups: sham mice given vehicle (Sham group, $n = 34$), bleomycin mice given vehicle (Vehicle group, $n = 34$), and bleomycin mice treated with ONO-1301 (ONO-1301 group, $n = 34$). Twenty-four additional mice were studied to evaluate the effect of ONO-1301 administration on survival in bleomycin mice. Twenty-five mice were studied to examine the effect of ONO-1301 on plasma cAMP. Finally, 15 mice were

Address for reprint requests and other correspondence: N. Nagaya, Dept. of Regenerative Medicine and Tissue Engineering, National Cardiovascular Center Research Inst., 5-7-1 Fujishirodai, Suita, Osaka 565-8565, Japan (e-mail: nnagaya@ri.ncvc.go.jp).

The costs of publication of this article were defrayed in part by the payment of page charges. The article must therefore be hereby marked "*advertisement*" in accordance with 18 U.S.C. Section 1734 solely to indicate this fact.

used to examine the effects of ONO-1301 on established pulmonary fibrosis. All protocols were performed in accordance with the guidelines of the Animal Care Ethics Committee of the National Cardiovascular Center Research Institute.

ONO-1301. We have recently developed a novel nonprostanoid long-acting prostacyclin agonist possessing a potent inhibitory activity against thromboxane synthase, {7,8-dihydro-5-[(E)-2-[(α-(3-pyridyl)benzylidene)amino-oxy]ethyl]-1-naphtyl-oxy} acetic acid, named ONO-1301 (Fig. 1). This compound has two interesting structural features. First, as stated above, unlike prostacyclin, ONO-1301 does not possess a five-membered ring and allylic alcohol in its molecule. This structural feature contributes to the biological and chemical stability of this compound. Second, this compound possesses a 3-pyridine moiety at one end of the molecule and a carboxylic acid group at the other. The inhibitory effect of ONO-1301 on thromboxane synthesis is mediated by binding of thromboxane synthase to 3-pyridine moiety and a carboxylic acid group in ONO-1301.

In vivo experimental protocol. After the mice were anesthetized by intraperitoneal injection of pentobarbital sodium, they were given intratracheal injection of either bleomycin (0.02 or 0.03 units/mouse) dissolved in 50 μl of saline or saline alone. Then, ONO-1301 (6 $mg \cdot kg^{-1} \cdot day^{-1}$) dissolved in 100 μl of saline, or saline was administered by subcutaneous injection twice a day throughout the experiment. This dose was determined to obtain maximum effects, based on dose-response experiments. Systolic blood pressure in the conscious state was measured by the indirect tail-cuff method with a blood pressure monitor (MK-2000; Muromachi Kikai, Tokyo, Japan) 0, 30, 60, 120, and 360 min after administration. ONO-1301 at a dose of 6 $mg \cdot kg^{-1} \cdot day^{-1}$ did not influence blood pressure. The mice were maintained under standard conditions with free access to food and water.

The effects of ONO-1301 on pulmonary fibrosis were analyzed by the following parameters: *1*) the severity of pulmonary fibrosis such as histological examination using the Ashcroft score and lung hydroxyproline content on *day 14* (0.02 units/mouse), *2*) the severity of acute lung injury such as that reflected in total cell count, differential cell count, and total protein level in bronchoalveolar lavage (BAL) fluid on *day 3* and *day 7* (0.02 units/mouse), *3*) TXB_2 and active transforming growth factor-β1 (TGF-β1) levels in BAL fluid on *day 3* and *day 7* (0.02 units/mouse), *4*) intracellular adhesion molecule-1 (ICAM-1) and vascular cell adhesion molecule-1 (VCAM-1) expression in whole lung tissue on *days 3* and *7* (0.02 units/mouse), and *5*) the survival rate on *day 21* (0.03 units/mouse).

Finally, to investigate the effects of ONO-1301 on established pulmonary fibrosis, 15 mice were randomly given an intratracheal injection of either bleomycin or saline. ONO-1301 or saline was administered from *day 14* to *28* (Sham, Vehicle, and ONO-1301 groups, $n = 5$ each). These mice were evaluated on *day 28*.

BAL analysis. Total and differential cell counts in BAL fluid were determined as described previously ($n = 5$ each) (20). The supernatant of BAL fluid was used for the measurement of total protein, TXB_2, which is a stable metabolite of TXA_2, and active TGF-β1 levels. The total protein level was measured by Bradford assay (Bio-Rad, Tokyo, Japan). The TXB_2 level was measured with an enzyme immunoassay kit (Cayman Chemical, Ann Arbor, MI). The active TGF-β1 level was measured with a mouse TGF-β1 ELISA kit (R&D Systems, Minneapolis, MN).

Histological examination. The right lung was fixed by inflation with 4% paraformaldehyde and embedded in paraffin ($n = 5$ each). Sections 4 μm thick were stained with hematoxylin-eosin. The Ashcroft score was used for semiquantitative assessment of fibrotic changes (1). The severity of fibrotic changes in each histological section of the lung was assessed as the mean score of severity from observed microscopic fields. Thirty fields in each section were analyzed. Grading was performed in a blinded fashion by three observers, and the mean was taken as the fibrosis score.

Measurement of hydroxyproline content. To quantify lung collagen content as an indicator of pulmonary fibrosis, the hydroxyproline content in the lung was measured in each group according to the previously described method ($n = 5$ each) (20). The left lung was quick-frozen and kept at −80°C until the assay. After the lung was homogenized, the suspension was hydrolyzed with 0.5 ml of 12 N hydrochloric acid for 20 h at 100°C. After neutralization, a 0.1 ml aliquot of supernatant was mixed in 1.5 ml of 0.3 N lithium hydroxide solution. The hydroxyproline content was analyzed by high-performance chromatography.

Quantification of ICAM-1 and VCAM-1 expression by ELISA. We investigated the effect of ONO-1301 on ICAM-1 and VCAM-1, which are key molecules in leukocyte migration into lung tissues, expression in the bleomycin-treated lung. The treated lungs were quick-frozen and kept at −80°C until the assay. The lungs were homogenized in 1.5 ml of saline. The homogenates were centrifuged at 2,000 *g* for 10 min at 4°C, and the supernatants were assayed for ICAM-1 and VCAM-1 concentrations by ELISA kits (R&D Systems).

Measurement of cAMP level. To evaluate the effect of ONO-1301 on plasma cAMP, normal mice were assigned to receive a single administration of ONO-1301 (3 mg/kg). Blood samples were obtained 0, 30, 60, 120, and 360 min after administration and were immediately transferred into a chilled glass tube containing disodium EDTA (1 mg/ml) and aprotinin (500 U/ml) and centrifuged immediately at 4°C

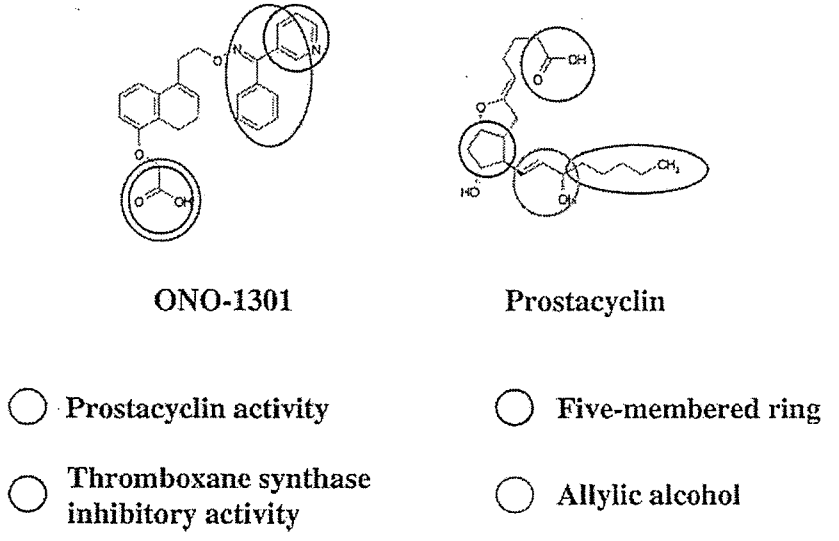

Fig. 1. Molecular structures of ONO-1301 and prostacyclin. Unlike prostacyclin, ONO-1301 does not possess a 5-membered ring and allylic alcohol, which contributes to the biological and chemical stability of this compound. ONO-1301 possesses a 3-pyridine moiety at 1 end of the molecule and a carboxylic acid group at the other, which contribute to inhibition of thromboxane synthesis. Green circle indicates prostacyclin activity; red circle indicates thromboxane synthase inhibitory activity; blue circle indicates 5-membered ring; orange circle indicates allylic alcohol.

Table 1. *Physiological profiles of three experimental groups*

	Sham	Vehicle	ONO-1301
n	8	8	8
Body weight, g	22.1±0.2	19.3±0.6*	21.8±0.4†
Lung weight/body weight, mg/g	5.8±0.1	14.8±1.7*	9.4±0.5*†

Data are means ± SE. These measurements were performed at 14 days after bleomycin injection. Sham, sham mice given vehicle; Vehicle, bleomycin mice given vehicle; ONO-1301, bleomycin mice treated with ONO-1301; *$P <$ 0.05 vs. Sham group; †$P < 0.05$ vs. Vehicle group.

($n = 5$ each). The plasma cAMP level was measured with a radioimmunoassay kit (Yamasa Shoyu, Chiba, Japan) as described previously (13).

Survival analysis. To evaluate the effect of ONO-1301 on survival in bleomycin-injected mice, 24 mice received repeated administration of ONO-1301 ($n = 12$) or vehicle ($n = 12$) for 21 days. Survival was estimated from the date of bleomycin injection to the death of the mouse or 21 days after injection.

In vitro study. Mouse lung fibroblasts were isolated from lung tissue by mincing and enzymatic digestion with collagenase type III (10 mg/lung; Worthington Biochemical, Lakewood, NJ) for 80 min at 37°C, as reported previously (11). Cell suspension was filtered through 70-μm filters (BD Biosciences, Mountain View, CA). Then, these cells were centrifuged, washed, and cultured in complete medium composed of DMEM (Invitrogen, Carlsbad, CA) supplemented with 10% fetal calf serum (FCS, Invitrogen) and 1% penicillin-streptomycin (Invitrogen). Fibroblasts were used after the first cell passage. To evaluate the effect of ONO-1301 on intracellular cAMP, mouse lung fibroblasts grown in 24-well plates were incubated with various concentrations of ONO-1301 in the presence of 5×10^{-4} M 3-isobutyl-1-methylxanthine (Nacalai Tesque, Kyoto, Japan), a phosphodiesterase inhibitor ($n = 8$ each), for 10 min. The intracellular cAMP level was measured with a radioimmunoassay kit as described previously (10). The effects of ONO-1301 and 8-bromo cAMP (Sigma, St. Louis, MO), a cAMP analog, on cell proliferation were assessed using a CellTiter 96 aqueous one solution cell proliferation assay kit (Promega, Madison, WI) according to the manufacturer's directions ($n = 8$ each). Cells were treated for 48 h with fresh medium containing 2.5% FCS along with various concentrations of ONO-1301 or 8-bromo cAMP. The effect of ONO-1301 (10^{-6} M) on cell proliferation in the presence of a myristoylated protein kinase A (PKA) inhibitor (10^{-6} M) (Protein Kinase A Inhibitor 14–22 Amide, Cell-permeable, Myristoylated; Calbiochem, Cambridge, MA) was also evaluated. Finally, to investigate the underlying mechanism responsible for regulation of cell proliferation, mouse lung-derived fibroblasts were treated with various concentrations of imidazole (Wako Pure Chemical Industries, Osaka, Japan), a thromboxane synthesis inhibitor, or beraprost sodium (Cayman Chemical), a stable prostacyclin analog.

Statistical analysis. All data are expressed as means ± SE unless otherwise indicated. Comparisons were made by one-way ANOVA followed by Newman-Keuls test. Survival curves were derived by the Kaplan-Meier method and compared by log-rank test. A value of $P <$ 0.05 was considered statistically significant.

RESULTS

Physiological profiles. The physiological profiles of the three experimental groups are shown in Table 1. Body weight was significantly lower in bleomycin mice given vehicle (Vehicle group) than in normal mice given vehicle (Sham group). However, a significant decrease in body weight was not observed in bleomycin mice treated with ONO-1301 (ONO-1301 group). Bleomycin injection significantly increased wet lung weight to body weight ratio. However, the increase was significantly attenuated by treatment with ONO-1301.

Inhibition of pulmonary fibrosis. The normal alveolar structure was maintained in the Sham group (Fig. 2*A*). Fourteen days after bleomycin injection, the alveolar walls were thickened and the air spaces were collapsed in the Vehicle group. In contrast to the findings in mice treated with bleomycin alone, pulmonary fibrosis was less severe in the ONO-1301 group. Semiquantitative assessment by the Ashcroft score demonstrated that the degree of pulmonary fibrosis in the ONO-1301 group was significantly lower than that in the Vehicle group (Fig. 2*B*). The hydroxyproline content in the lung was significantly increased after bleomycin injection (Fig. 2*C*). However,

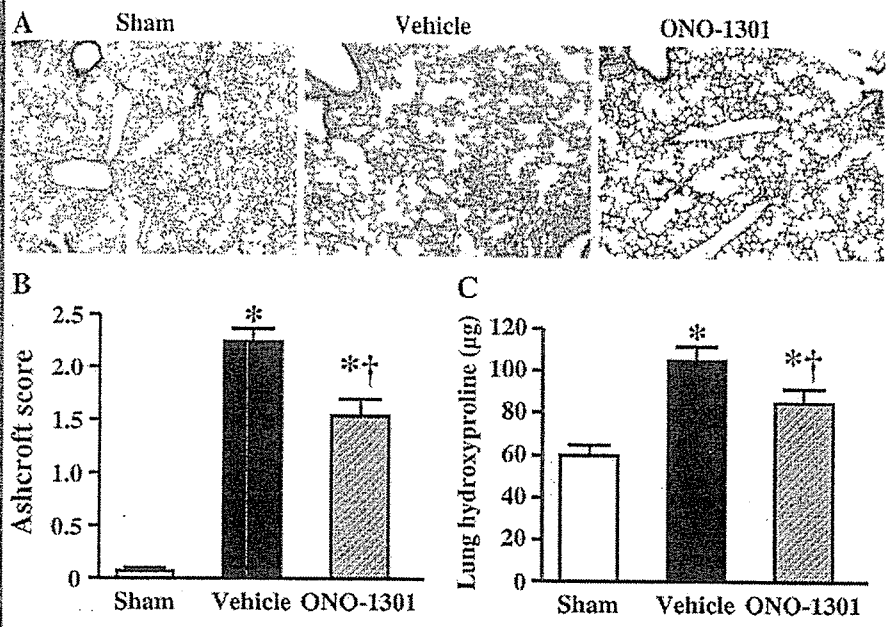

Fig. 2. *A*: representative photomicrographs of lung tissue at 14 days after bleomycin injection. Bleomycin-induced pulmonary fibrosis was attenuated by treatment with ONO-1301. Hematoxylin-eosin stain; magnification ×100. *B*: semiquantitative analyses of lung tissue using the Ashcroft score, a marker for pulmonary fibrosis. *C*: effect of ONO-1301 administration on hydroxyproline content in left lung of bleomycin-injected mice. Data are means ± SE. *$P <$ 0.05 vs. Sham group; †$P < 0.05$ vs. Vehicle group.

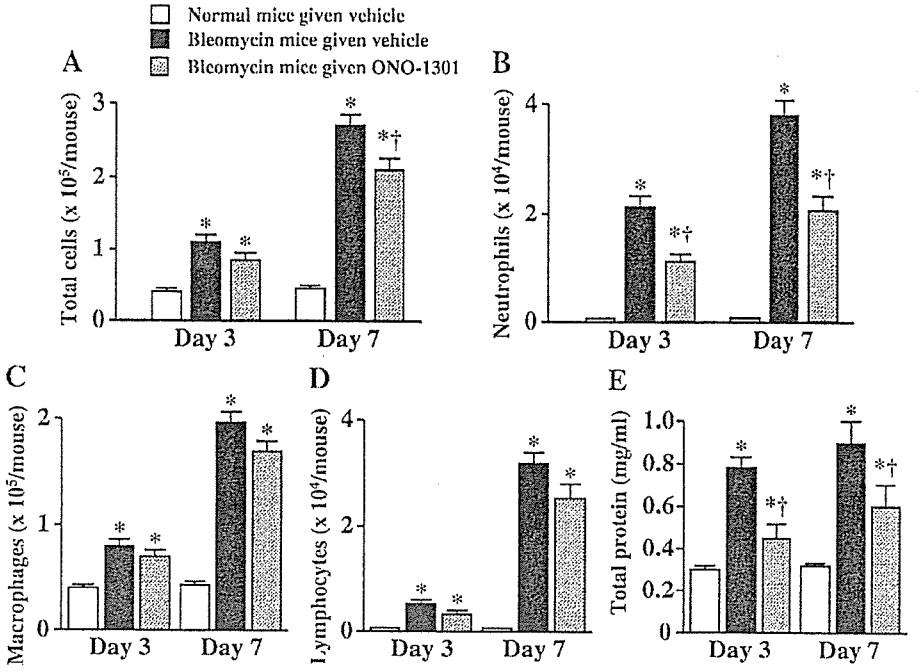

Fig. 3. Effects of ONO-1301 administration on total and differential cell counts (macrophages, *C*; lymphocytes, *D*) in bronchoalveolar lavage (BAL) fluid at 3 and 7 days after bleomycin injection. ONO-1301 significantly inhibited the increases in total cell count at 7 days (*A*) and neutrophil count at 3 and 7 days (*B*) after bleomycin injection. *E*: effect of ONO-1301 administration on total protein level in BAL fluid at 3 and 7 days after bleomycin injection. ONO-1301 significantly inhibited the increase in total protein level in BAL fluid. Data are means ± SE. $*P < 0.05$ vs. Sham group, $\dagger P < 0.05$ vs. Vehicle group.

subcutaneous administration of ONO-1301 significantly decreased the hydroxyproline content in bleomycin-injected mice.

Attenuation of lung inflammation. The recovery rate of BAL fluid was >85% in all groups. Total and differential cell counts were increased at 3 and 7 days after bleomycin injection (Fig. 3, *A–D*). However, subcutaneous administration of ONO-1301 significantly attenuated the increases in total cell count at 7 days and neutrophil count at 3 and 7 days after bleomycin injection. ONO-1301 administration tended to attenuate the increases in macrophage and lymphocyte counts, although these changes did not reach statistical significance. The total protein level was significantly increased at 3 and 7 days after bleomycin injection (Fig. 3*E*). However, the increase was significantly inhibited by ONO-1301.

Inhibition of thromboxane synthesis. The TXB_2 level in BAL fluid was significantly increased at 3 and 7 days after bleomycin injection (Fig. 4*A*), suggesting a pathological role of thromboxane in bleomycin-injected mice. Subcutaneous administration of ONO-1301 markedly inhibited the increase in TXB_2 level. The active TGF-β1 level in BAL fluid was significantly increased at 7 days after bleomycin injection (Sham group, 148 ± 6; Vehicle group, 251 ± 8; ONO-1301 group, 238 ± 9 pg/ml). ONO-1301 did not significantly alter the active TGF-β1 level in BAL fluid.

Inhibitory effect of ONO-1301 on ICAM-1 and VCAM-1 expression. The lung ICAM-1 and VCAM-1 levels were significantly increased at 3 and 7 days after bleomycin injection (Fig. 4, *B* and *C*). ONO-1301 administration sig-

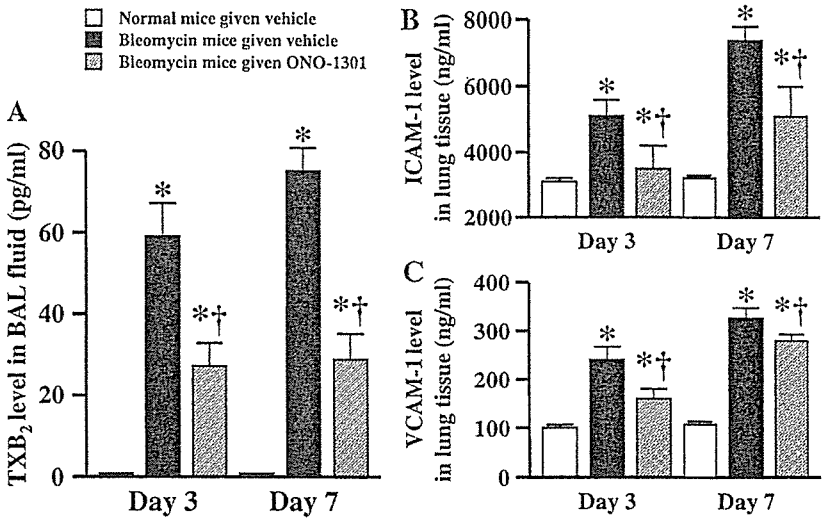

Fig. 4. *A*: effect of ONO-1301 administration on thromboxane B_2 (TXB_2) level in BAL fluid at 3 and 7 days after bleomycin injection. ONO-1301 markedly inhibited the increase in TXB_2 level in BAL fluid. Data are means ± SE. Effects of ONO-1301 administration on ICAM-1 (*B*) and VCAM-1 (*C*) levels in lung tissue at 3 and 7 days after bleomycin injection. $*P < 0.05$ vs. Sham group, $\dagger P < 0.05$ vs. Vehicle group.

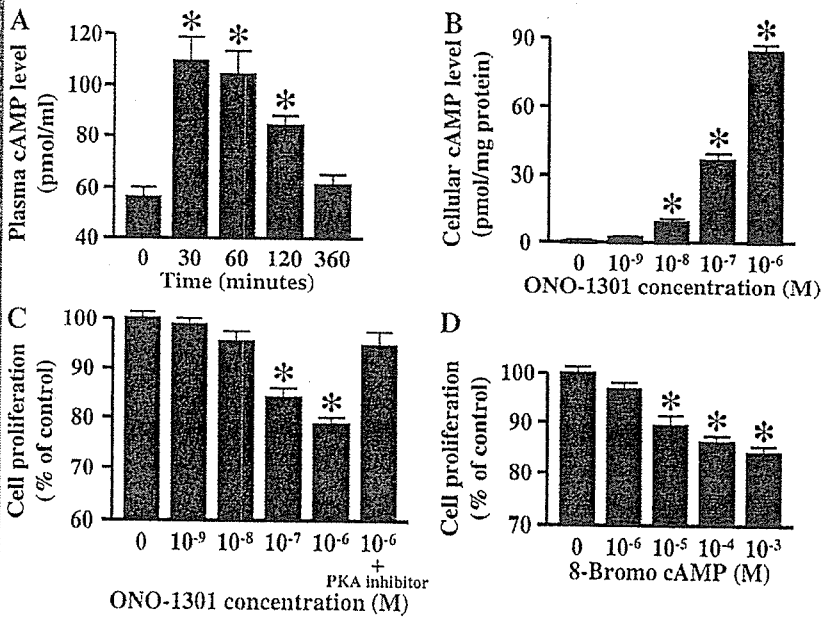

Fig. 5. *A*: time course of plasma cAMP level after a single subcutaneous administration of ONO-1301. *B*: dose-dependent effects of ONO-1301 on intracellular cAMP level. *C*: effect of ONO-1301 on fibroblast proliferation. ONO-1301 significantly reduced cell proliferation at concentrations of 10^{-7} M or greater, and this inhibitory effect was attenuated by a protein kinase A (PKA) inhibitor. *D*: effect of 8-bromo cAMP on fibroblast proliferation. Data are means ± SE. $*P < 0.05$ vs. Control.

nificantly attenuated the increases in ICAM-1 and VCAM-1 levels.

Activation of the cAMP/PKA pathway. A single subcutaneous administration of ONO-1301 significantly increased plasma cAMP level (Fig. 5*A*). The increase lasted longer than 2 h. In vitro, ONO-1301 dose-dependently increased intracellular cAMP level in mouse lung fibroblasts (Fig. 5*B*). ONO-1301 significantly reduced proliferation of mouse lung fibroblasts at concentrations of 10^{-7} M or greater, and this inhibitory effect was attenuated by a PKA inhibitor (Fig. 5*C*). The reduction in cell proliferation by ONO-1301 was reproduced by 8-bromo cAMP (Fig. 5*D*). Beraprost sodium (10^{-7} M) significantly reduced fibroblast proliferation (86% of control). However, imidazole at different concentrations (10^{-6}-10^{-9} M) did not significantly regulate cell proliferation.

Survival analysis. Kaplan-Meier survival curves demonstrated that bleomycin mice treated with ONO-1301 had a significantly higher survival rate than those given vehicle (75 vs. 33% 21-day survival, log-rank test, $P < 0.05$, Fig. 6).

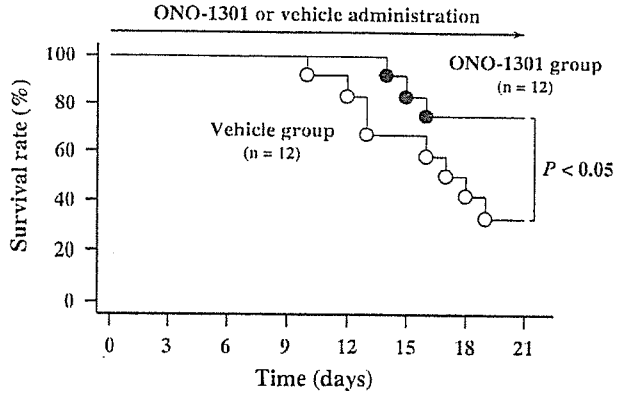

Fig. 6. Kaplan-Meier survival curves. Bleomycin mice treated with ONO-1301 (●) had a significantly higher survival rate than those given vehicle (○) (log-rank test, $P < 0.05$).

Delayed therapy. There were no significant differences in Ashcroft score and lung hydroxyproline content between the Vehicle group and ONO-1301 group at 28 days after bleomycin injection (data not shown).

DISCUSSION

In the present study, we demonstrated that *1*) repeated subcutaneous administration of ONO-1301 attenuated the development of bleomycin-induced pulmonary fibrosis, as indicated by decreases in Ashcroft score and lung hydroxyproline content, *2*) ONO-1301 attenuated the increases in total cell count, neutrophil count, and total protein level in BAL fluid, and *3*) ONO-1301 increased the survival rate in bleomycin-injected mice. We also demonstrated that *4*) ONO-1301 decreased the TXB_2 level in BAL fluid and inhibited ICAM-1 and VCAM-1 expression in the bleomycin-treated lung, and *5*) ONO-1301 inhibited lung fibroblast proliferation through activation of the cAMP/PKA pathway.

The balance between prostacyclin and TXA_2 plays an important role in pulmonary homeostasis. However, little information is available regarding the therapeutic potency of these prostanoids for pulmonary fibrosis. Recently, we have developed ONO-1301, a novel nonprostanoid long-acting prostacyclin agonist possessing a potent inhibitory activity against thromboxane synthase. Thus this compound was administered by subcutaneous injection twice a day.

Bleomycin induces lung inflammation followed by fibrosis when intratracheally injected in experimental animals (27). In the present study, subcutaneous administration of ONO-1301 significantly attenuated bleomycin-induced increases in total cell counts, neutrophil counts, and total protein level in BAL fluid. Earlier studies have shown that TXA_2 acts as a proinflammatory mediator via enhancement of pulmonary vascular permeability (18, 24) and neutrophil adhesion (33). In the present study, TXB_2, a stable metabolite of TXA_2, was significantly increased after bleomycin injection, which is consistent with previous studies (2, 8). However, ONO-1301 markedly

inhibited the increase in TXB_2 level in BAL fluid. Thus one of the possible mechanisms by which ONO-1301 attenuates lung inflammation may be mediated by inhibition of TXA_2 synthesis. A recent study has shown that a TXA_2 receptor agonist enhances the expression of adhesion molecules by human vascular endothelial cells (12). In the present study, ONO-1301 significantly inhibited ICAM-1 and VCAM-1 expression in the bleomycin-treated lung. Adhesion molecules including ICAM-1 and VCAM-1 have been shown to contribute to bleomycin-induced pulmonary fibrosis by mediating the accumulation of leukocytes (9, 16, 19, 23). These findings suggest that ONO-1301 may attenuate lung inflammation at least in part through inhibition of ICAM-1 and VCAM-1 expression.

Lung fibroblasts play an important role in the development of fibrosis in the lung (22, 25, 31). Prostaglandins are known to have various functions on lung fibroblasts via an elevation of intracellular cAMP level (3, 14–17). In the present study, a single subcutaneous administration of ONO-1301 significantly increased plasma cAMP level in mice. In vitro studies demonstrated that ONO-1301 dose-dependently increased intracellular cAMP level in mouse lung fibroblasts and that this compound dose-dependently inhibited fibroblast proliferation. The inhibitory effect of ONO-1301 was reproduced by 8-bromo cAMP, a cAMP analog, and attenuated by a PKA inhibitor. These results suggest that ONO-1301 directly inhibits fibroblast proliferation at least in part through activation of the cAMP/PKA pathway. Dussaubat et al. (5) have demonstrated that imidazole, a thromboxane synthesis inhibitor, decreases bleomycin-induced acute lung inflammation, but it does not affect pulmonary fibrosis at later points. In the present study, a prostacyclin analog, but not a thromboxane synthesis inhibitor, significantly reduced fibroblast proliferation. These results suggest that the inhibitory effect of ONO-1301 on fibroblast proliferation may be mediated mainly by its prostacyclin-like activity. TGF-β, especially TGF-β1 plays an important role in the pathogenesis of pulmonary fibrosis (7, 26, 32). In the present study, ONO-1301 did not significantly alter the active TGF-β1 level in BAL fluid. Previous studies have shown that a prostacyclin agonist suppresses TGF-β-induced connective tissue growth factor, a potent profibrotic mediator, expression in part through activation of the cAMP/PKA pathway (28, 29). Thus it is interesting to speculate that ONO-1301 attenuated the development of pulmonary fibrosis through suppression of connective tissue growth factor.

In the present study, ONO-1301 significantly improved survival in bleomycin-injected mice. ONO-1301 inhibited lung inflammation and lung fibroblast proliferation. As a result, ONO-1301 may have beneficial effects on survival in bleomycin-injected mice. Unfortunately, we could not observe significant differences in fibrotic changes between the Vehicle group and ONO-1301 group when we administered ONO-1301 after fibrosis was established. These results imply that ONO-1301 may be insufficient to reverse established pulmonary fibrosis.

In conclusion, subcutaneous administration of ONO-1301, a novel long-lasting prostacyclin agonist, attenuated the development of bleomycin-induced pulmonary fibrosis and improved survival in mice. The beneficial effects were mediated at least in part by inhibition of TXA_2 synthesis and activation of the cAMP/PKA pathway. Thus administration of this compound may be a new therapeutic strategy for the treatment of pulmonary fibrosis.

ACKNOWLEDGMENTS

The authors thank Yuki Isono, Natue Sakata, and Manami Sone for excellent technical assistance.

GRANTS

This work was supported by grants from Ono Pharmaceutical Co., Ltd.

REFERENCES

1. **Ashcroft T, Simpson JM, and Timbrell V.** Simple method of estimating severity of pulmonary fibrosis on a numerical scale. *J Clin Pathol* 41: 467–470, 1988.
2. **Chandler DB, Giri SN, Chen Z, and Hyde DM.** The in vitro synthesis and degradation of prostaglandins during the development of bleomycin-induced pulmonary fibrosis in hamsters. *Prostaglandins Leukot Med* 11: 11–31, 1983.
3. **Clark JG, Kostal KM, and Marino BA.** Bleomycin-induced pulmonary fibrosis in hamsters. An alveolar macrophage product increases fibroblast prostaglandin E2 and cyclic adenosine monophosphate and suppresses fibroblast proliferation and collagen production. *J Clin Invest* 72: 2082–2091, 1983.
4. **Cruz-Gervis R, Stecenko AA, Dworski R, Lane KB, Loyd JE, Pierson R, King G, and Brigham KL.** Altered prostanoid production by fibroblasts cultured from the lungs of human subjects with idiopathic pulmonary fibrosis. *Respir Res* 3: 17, 2002.
5. **Dussaubat N, Capetillo M, Lathrop ME, Mendoza R, and Oyarzun M.** The effects of imidazole on pulmonary damage induced by bleomycin. *Biol Res* 28: 261–266, 1995.
6. **Giri SN.** Novel pharmacological approaches to manage interstitial lung fibrosis in the twenty-first century. *Annu Rev Pharmacol Toxicol* 43: 73–95, 2003.
7. **Giri SN, Hyde DM, and Hollinger MA.** Effect of antibody to transforming growth factor beta on bleomycin induced accumulation of lung collagen in mice. *Thorax* 48: 959–966, 1993.
8. **Giri SN and Witt TC.** Effects of intratracheal administration of bleomycin on prostaglandins and thromboxane-B2 and collagen levels of the lung in hamsters. *Exp Lung Res* 9: 119–133, 1985.
9. **Hamaguchi Y, Nishizawa Y, Yasui M, Hasegawa M, Kaburagi Y, Komura K, Nagaoka T, Saito E, Shimada Y, Takehara K, Kadono T, Steeber DA, Tedder TF, and Sato S.** Intercellular adhesion molecule-1 and L-selectin regulate bleomycin-induced lung fibrosis. *Am J Pathol* 161: 1607–1618, 2002.
10. **Horio T, Nishikimi T, Yoshihara F, Matsuo H, Takishita S, and Kangawa K.** Inhibitory regulation of hypertrophy by endogenous atrial natriuretic peptide in cultured cardiac myocytes. *Hypertension* 35: 19–24, 2000.
11. **Huaux F, Liu T, McGarry B, Ullenbruch M, and Phan SH.** Dual roles of IL-4 in lung injury and fibrosis. *J Immunol* 170: 2083–2092, 2003.
12. **Ishizuka T, Kawakami M, Hidaka T, Matsuki Y, Takamizawa M, Suzuki K, Kurita A, and Nakamura H.** Stimulation with thromboxane A2 (TXA2) receptor agonist enhances ICAM-1, VCAM-1 or ELAM-1 expression by human vascular endothelial cells. *Clin Exp Immunol* 112: 464–470, 1998.
13. **Itoh T, Nagaya N, Fujii T, Iwase T, Nakanishi N, Hamada K, Kangawa K, and Kimura H.** A combination of oral sildenafil and beraprost ameliorates pulmonary hypertension in rats. *Am J Respir Crit Care Med* 169: 34–38, 2004.
14. **Kohyama T, Liu X, Kim HJ, Kobayashi T, Ertl RF, Wen FQ, Takizawa H, and Rennard SI.** Prostacyclin analogs inhibit fibroblast migration. *Am J Physiol Lung Cell Mol Physiol* 283: L428–L432, 2002.
15. **Kolodsick JE, Peters-Golden M, Larios J, Toews GB, Thannickal VJ, and Moore BB.** Prostaglandin E2 inhibits fibroblast to myofibroblast transition via E. prostanoid receptor 2 signaling and cyclic adenosine monophosphate elevation. *Am J Respir Cell Mol Biol* 29: 537–544, 2003.
16. **Li Y, Azuma A, Takahashi S, Usuki J, Matsuda K, Aoyama A, and Kudoh S.** Fourteen-membered ring macrolides inhibit vascular cell adhesion molecule 1 messenger RNA induction and leukocyte migration: role in preventing lung injury and fibrosis in bleomycin-challenged mice. *Chest* 122: 2137–2145, 2002.
17. **Liu X, Ostrom RS, and Insel PA.** cAMP-elevating agents and adenylyl cyclase overexpression promote an antifibrotic phenotype in pulmonary fibroblasts. *Am J Physiol Cell Physiol* 286: C1089–C1099, 2004.

18. **Lotvall J, Elwood W, Tokuyama K, Sakamoto T, Barnes PJ, and Chung KF.** A thromboxane mimetic, U-46619, produces plasma exudation in airways of the guinea pig. *J Appl Physiol* 72: 2415–2419, 1992.
19. **Matsuse T, Teramoto S, Katayama H, Sudo E, Ekimoto H, Mitsuhashi H, Uejima Y, Fukuchi Y, and Ouchi Y.** ICAM-1 mediates lung leukocyte recruitment but not pulmonary fibrosis in a murine model of bleomycin-induced lung injury. *Eur Respir J* 13: 71–77, 1999.
20. **Murakami S, Nagaya N, Itoh T, Fujii T, Iwase T, Hamada K, Kimura H, and Kangawa K.** C-type natriuretic peptide attenuates bleomycin-induced pulmonary fibrosis in mice. *Am J Physiol Lung Cell Mol Physiol* 287: L1172–L1177, 2004.
21. **Murota SI, Morita I, and Abe M.** The effects of thromboxane B2 and 6-ketoprostaglandin F1alpha on cultured fibroblasts. *Biochim Biophys Acta* 479: 122–125, 1977.
22. **Kaminski N, Belperio JA, Bitterman PB, Chen L, Chensue SW, Choi AM, Dacic S, Dauber JH, Du Bois RM, Enghild JJ, Fattman CL, Grutters JC, Haegens A, Hanford LE, Heintz N, Henson PM, Hogaboam C, Kagan VE, Keane MP, Kunkel SL, Land S, Loyd JE, Lukacs N, MacPherson M, Manning B, Manning N, Martinelli M, Moller DR, Morse D, Mossman B, Noble PW, Nowak N, Oury TD, Pardo A, Perez A, Petty TL, Phan SH, Ramos-Nino ME, Ray P, Rogers RM, Sato H, Scapoli L, Schaefer LM, Selman M, Stern M, Strollo DC, Tyurin VA, Valnickova Z, Welsh KI, Witzmann FA, Yousem SA, and Strieter RM.** Idiopathic pulmonary fibrosis. *Am J Respir Cell Mol Biol* 29: S1–S105, 2003.
23. **Sato N, Suzuki Y, Nishio K, Suzuki K, Naoki K, Takeshita K, Kudo H, Miyao N, Tsumura H, Serizawa H, Suematsu M, and Yamaguchi K.** Roles of ICAM-1 for abnormal leukocyte recruitment in the microcirculation of bleomycin-induced fibrotic lung injury. *Am J Respir Crit Care Med* 161: 1681–1688, 2000.
24. **Schulman CI, Wright JK, Nwariaku F, Sarosi G, and Turnage RH.** The effect of tumor necrosis factor-alpha on microvascular permeability in an isolated, perfused lung. *Shock* 18: 75–81, 2002.
25. **Sheppard D.** Pulmonary fibrosis: a cellular overreaction or a failure of communication? *J Clin Invest* 107: 1501–1502, 2001.
26. **Sime PJ, Xing Z, Graham FL, Csaky KG, and Gauldie J.** Adenovector-mediated gene transfer of active transforming growth factor-beta1 induces prolonged severe fibrosis in rat lung. *J Clin Invest* 100: 768–776, 1997.
27. **Snider GL, Hayes JA, and Korthy AL.** Chronic interstitial pulmonary fibrosis produced in hamsters by endotracheal bleomycin: pathology and stereology. *Am Rev Respir Dis* 117: 1099–1108, 1978.
28. **Stratton R, Rajkumar V, Ponticos M, Nichols B, Shiwen X, Black CM, Abraham DJ, and Leask A.** Prostacyclin derivatives prevent the fibrotic response to TGF-beta by inhibiting the Ras/MEK/ERK pathway. *FASEB J* 16: 1949–1951, 2002.
29. **Stratton R, Shiwen X, Martini G, Holmes A, Leask A, Haberberger T, Martin GR, Black CM, and Abraham D.** Iloprost suppresses connective tissue growth factor production in fibroblasts and in the skin of scleroderma patients. *J Clin Invest* 108: 241–250, 2001.
30. **Tanouchi T, Kawamura M, Ohyama I, Kajiwara I, Iguchi Y, Okada T, Miyamoto T, Taniguchi K, Hayashi M, Iizuka K, and Nakazawa M.** Highly selective inhibitors of thromboxane synthetase. 2 Pyridine derivatives. *J Med Chem* 24: 1149–1155, 1981.
31. **Uhal BD, Joshi I, True AL, Mundle S, Raza A, Pardo A, and Selman M.** Fibroblasts isolated after fibrotic lung injury induce apoptosis of alveolar epithelial cells in vitro. *Am J Physiol Lung Cell Mol Physiol* 269: L819–L828, 1995.
32. **Wang Q, Wang Y, Hyde DM, Gotwals PJ, Koteliansky VE, Ryan ST, and Giri SN.** Reduction of bleomycin induced lung fibrosis by transforming growth factor beta soluble receptor in hamsters. *Thorax* 54: 805–812, 1999.
33. **Wiles ME, Welbourn R, Goldman G, Hechtman HB, and Shepro D.** Thromboxane-induced neutrophil adhesion to pulmonary microvascular and aortic endothelium is regulated by CD18. *Inflammation* 15: 181–199, 1991.

TISSUE ENGINEERING
Volume 12, Number 6, 2006

Technical Report

Assessment of Viability and Osteogenic Ability of Human Mesenchymal Stem Cells After Being Stored in Suspension for Clinical Transplantation

KAORI MURAKI, B.Sc.,[1] MOTOHIRO HIROSE, Ph.D.,[1] NORIKO KOTOBUKI, Ph.D.,[1] YOICHI KATO, B.Sc.,[1] HIROKO MACHIDA, M.Sc.,[1]YOSHINORI TAKAKURA, M.D.,[2] and HAJIME OHGUSHI, M.D.[1]

ABSTRACT

Human mesenchymal stem cells (MSCs) were suspended in phosphate-buffered saline (PBS) and stored up to 24 h at 4°C, 24°C, and 37°C. More than 80% viability was maintained at any temperature for at least 1 h, then gradually decreased over time. After 24 h, the viabilities at 4°C, 24°C, and 37°C were about 81%, 70%, and 62%, respectively. The MSCs suspended/stored in PBS at 4°C for 24 h also exhibited *in vitro* osteogenic differentiation capability as evidenced by mineralized matrix formation as well as high alkaline phosphatase activity when cultured in an osteogenic medium. Furthermore, *in vivo* implantation experiments using the MSCs also demonstrated new bone formation. Because MSCs are known to possess multipotential stem cell characteristics, these data indicate that human MSCs stored in PBS at 4°C could be delivered to distant medical facilities for the purpose of hard tissue and other types of tissue regeneration therapy.

INTRODUCTION

MARROW STROMAL STEM CELLS,[1] recently termed "mesenchymal stem cells (MSCs)"[2] are highly proliferative cells that can be maintained in culture and readily differentiated into mesodermal cell types (fat, bone, cartilage and muscle).[1–3] Many researchers including us have previously reported that human MSCs derived from bone marrow differentiate into osteoblasts by *in vivo* implantation.[4,5] The osteogenic potential of MSCs has already been applied in clinical situations. Horwitz used allogenic MSCs for the treatment of osteogenesis imperfecta,[6] and Quarto *et al.*[7] used autogenous MSCs/ceramic composites for treatments of fractures. The MSCs can also differentiate into osteoblasts by *in vitro* culture with dexamethasone (Dex).[8–10] The *in vitro* differentiation resulted in osteoblastic phenotype expression of MSCs, and the osteoblasts formed extracellular bone matrices with abundant minerals on various culture substrata including ceramic surfaces.[11,12] The *in vitro*-formed osteoblasts/bone matrix on ceramic surface has been used for the treatment of osteoarthritic cases.[13,14] Recent studies have

[1]Tissue Engineering Research Group, Research Institute for Cell Engineering (RICE), National Institute of Advanced Industrial Science and Technology (AIST) Hyogo, Japan.
[2]Department of Orthopedic Surgery, Nara Medical University Nara, Japan.

also shown the possibility that MSCs can differentiate not only into the variety of mesodermal cells, but also into either ectodermal or endodermal cells.[15–20] This ability indicates the usefulness of MSCs for tissue engineering.

As therapies advanced from research laboratories to actual clinical applications, tissue regeneration using MSCs should be considered from practical viewpoints such as the maintenance and transportation of highly functional MSCs. However, optimal storage conditions have not been extensively investigated, especially for MSCs stored in liquid suspension, which could be available as ready-to-use cellular devices.

In this study, we investigated the viability of MSCs suspended in phosphate-buffered saline (PBS) at three different temperatures after storage from 0 to 24 h. We also observed the cell surface antigens and further examined the *in vitro* as well as *in vivo* osteogenic differentiation capability of the MSCs.

MATERIALS AND METHODS

Preparation and culture of marrow cells

Human bone marrow was aspirated from the iliac crest of three donors (16-year-old girl, 26-year-old man, and 29-year-old woman) with informed consent. Three milliliters of the marrow aspirates were immediately collected into a syringe containing 3 mL of PBS (phosphate buffered saline minus Ca^{2+} and Mg^{2+}, Invitrogen Corp., Carlsbad, CA) composed of 0.2 g/L KCl, 0.2 g/L KH_2PO_4, 8.0 g/L NaCl, and 2.16 g/L Na_2HPO_4 and 30 IU of heparin. After centrifugation at 140 ×g for 10 min at 4°C, the supernatants of the plasma and fat layers were discarded. The remaining nucleated cells with the red blood cell layer were seeded/divided into two T-75 flasks (Becton Dickinson Co., NJ) with 15 mL of medium. The culture medium was Eagle's minimum essential medium alpha (α-MEM, Invitrogen Corp.) containing 15% fetal bovine serum (FBS, JRH Biosciences Inc., KS) and antibiotics (100 U/mL penicillin G, 100 μg/mL streptomycin sulfate, and 0.25 μg/mL amphotericin B; Sigma-Aldrich Corp., MO). Primary cultures were maintained in a humidified atmosphere of 5% CO_2 at 37°C. Culture media were renewed two or three times per week. At each medium change, nonadherent red blood cells and hematopoietic cells could be removed. After 10 days, adherent cells became almost confluent.[14]

The adherent cells showed high capability for proliferation and differentiation. Analyses of the cell surface antigens revealed the absence of hematopoietic markers but the presence of mesenchymal cell markers.[21] Therefore, we refer to the cells as mesenchymal stem cells (MSCs) in this article. The cells were released from the substrates using a solution of 0.05 (w/v)% trypsin/0.53 mM EDTA (Invitrogen Corp). The harvested cells were centrifuged to concentrate at a density of 5×10^5 cells/mL in solution for cryopreservation (Cell Banker, Juji Field, Inc., Tokyo, Japan) and frozen at –80°C before use. After thawing, the cryopreserved MSCs attached and proliferated well on the culture dish surface, and their proliferation/differentiation capability was comparable to that of noncryopreserved MSCs.[22]

Cell viability assay

The viability of MSCs was assayed using a NucleoCounter (ChemoMetec, Allerød, Denmark), an instrument for counting mammalian cells, which was equipped with a fluorescence microscope. The cell count system is based on propidium iodide (PI) staining[23] to detect nonviable cells, because the PI only penetrates cells having damaged membranes and binds to DNA. After an additional procedure of complete cell lyses, the PI can bind to DNA in all cells, thus enabling determination of the total number of cells.

After immediate thawing of the frozen MSCs, 5×10^5 of the cells were cultured in a 90-mm^2 tissue culture dish for 7 to 10 days to reach near confluence. After the cells were released by trypsin digestion, the cells at a concentration of 1×10^6 cells/mL were suspended in 600 μL of PBS, and stored for periods from 0 h (immediately used) to 24 h at 4°C, 24°C, and 37°C. To determine viability, 40 μL of each sample diluted five times with PBS was analyzed using the NucleoCounter, giving an estimate of nonviable and total cells.

Although the NucleoCounter provides information of nonviable and total cell number, direct visualization of viable and nonviable cells at the cellular level cannot be

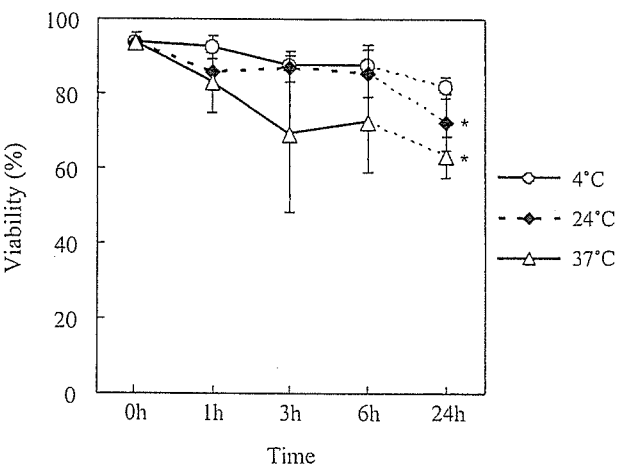

FIG. 1. Percent of viable MSCs stored in PBS at 4°C, 24°C, and 37°C from 0 h to 24 h. The data represent the mean ± SD of the six samples. *$p < 0.05$; significant difference against the viability of the cells stored in PBS at 4°C.

done. To visualize the cells, a LIVE/DEAD Viability Assay Kit (Molecular Probes, Inc., OR) was used to determine the numbers of living and dead cells at the same moment with calcein-AM for intracellular esterase and ethidium homodimer-1(EthD-1) for plasma membrane integrity.

MSCs suspended/stored in PBS at 4°C, 24°C, and 37°C were sampled in the dishes at each time point (0 h, 1 h, 3 h, 6 h, and 24 h), and 2 mM of calcein-AM and 5 mM of EthD-1 in PBS were directly added to the sampled cells at room temperature. After 15 min, the samples were observed by using a fluorescence microscope (IX70, OLYMPUS Co. Ltd., Tokyo, Japan).

Immunostaining and FACS analysis

MSCs suspended/stored in PBS at 4°C, 24°C or 37°C for 24 h were diluted into 1.5-mL centrifuge tubes and incubated with antibodies on ice for 15 min. The cells were pelleted, washed twice in PBS, and analyzed by a FACSCalibur flow cytometer (Becton Dickinson Co.). The antibodies used were CD13-FITC (fluorescein isothiocyanate), CD45-FITC (BIOCARTA Europe, Hamburg, Germany), and CD34-FITC (CARTAG Laboratories, CA).

Osteogenic differentiation assay

MSCs suspended/stored in PBS at 4°C for each time period (0, 1, 3, 6, and 24 h) were seeded at a cell density of 1×10^4 cells/cm^2 in a 12-well culture plate and cultured in media supplemented with 15% FBS, 10 mM β-glycerophosphate (affiliate of Merck KGaA, Darmstadt, Germany), disodium salt, 0.07 mM L-ascorbic acid phosphate (Sigma-Aldrich Corp.), and 0.1 μM dexamethasone (Dex) (Sigma-Aldrich Corp.) for 2 or 3 weeks. Because Dex is known as an osteogenic factor to MSCs,[8,9,21,22] cultures without Dex were used as a negative control. To enable the detection of the mineralized extracellular matrix, 1 μg/mL of calcein (Dojindo Laboratories, Kumamoto, Japan) was added at every media change. After culture for 14 days, the cell layers were washed twice with

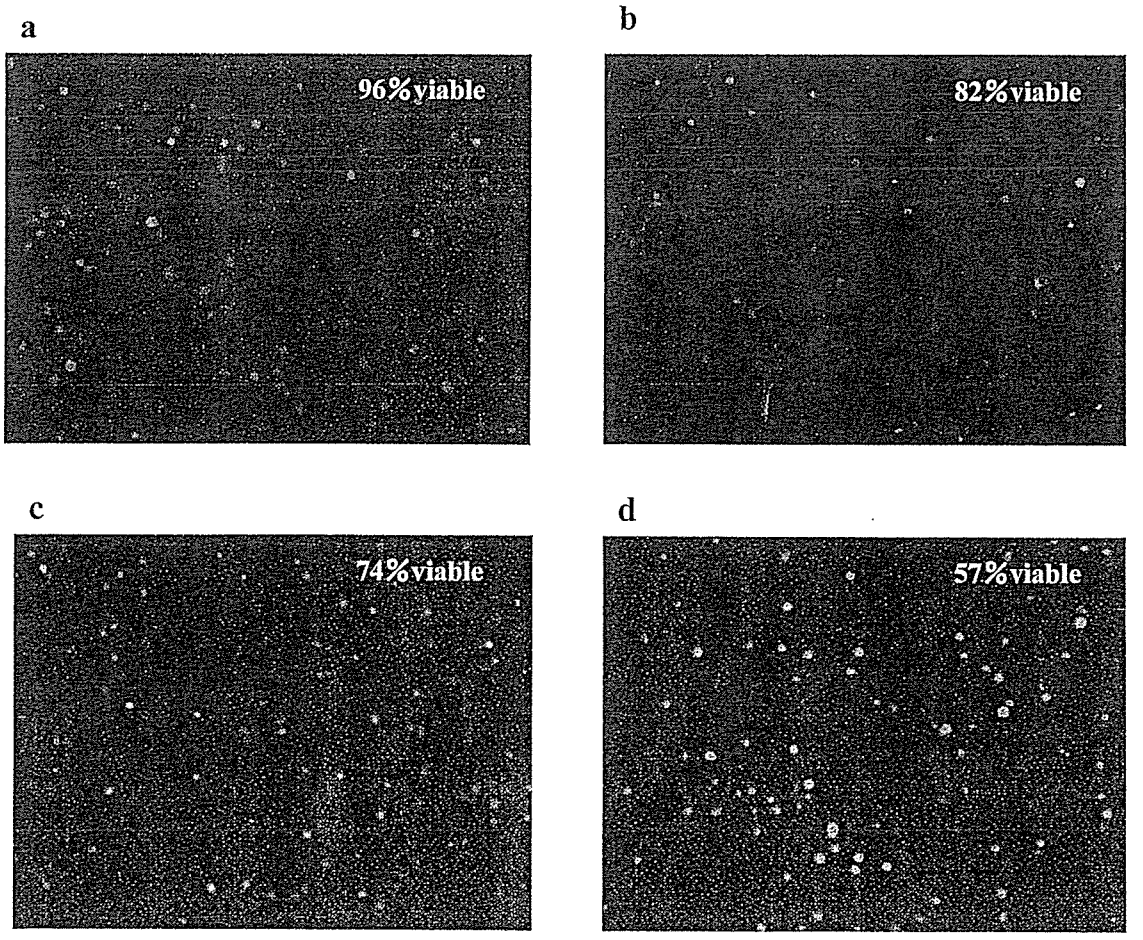

FIG. 2. Fluorescence microscopic view of MSCs stored in PBS after LIVE/DEAD Viability assay. **(a)** Immediately visualized with no storage, **(b)** stored at 4°C for 24 h, **(c)** stored at 24°C for 24 h, and **(d)** stored at 37°C for 24 h. Green fluorescent signal indicates living cells and red fluorescent signal indicates dead cells.

PBS, and then the fluorescence of the deposited calcein was visualized and quantified by using an image analyzer (Typhoon 8600, Molecular Dynamics, Inc., Sunnyvale, CA).[24] The fluorescent intensities parallel well the contents of calcium in the mineralized matrix.[24] Human fibroblasts (2F0-C25, Cell Systems, CA) were also used as negative controls against MSCs. Human fibroblasts stored at 4°C for 24 h were seeded at a cell density of 1×10^4 cells/cm^2 in a 12-well culture plate and cultured in media comprising 15% FBS, 10 mM β-glycerophosphate, disodium salt, 0.07 mM L-ascorbic acid phosphate, 0.1 μM Dex, and 1 μg/mL calcein. After culture for 21 days, the cell layers were washed twice with PBS, and the fluorescence of the deposited calcein was visualized and quantified by using an image analyzer.

To measure ALP activity, the cell layers from each well were collected into 0.5 mL of 10 mM Tris-buffer (pH 7.4, 1 mM EDTA, 100 mM NaCl) by scraping. The scraped cells were then sonicated and centrifuged at 13,000 $\times$g for 1 min at 4°C. An aliquot (20 μL) of the supernatant was assayed for ALP (alkaline phosphatase) activity using a *p*-nitrophenyl phosphate substrate (Zymed Laboratories Inc., CA).[9,11] The ALP activity was represented by *p*-nitrophenol, which was released after incubation for 30 min at 37°C. In the case of *in vivo* study, implants as described below were homogenized and sonicated in the above buffer solution prior to the ALP activity assay.

Implantation of MSCs/ HA constructs into athymic nude rats

MSCs suspended/stored in PBS at 4°C for 0 h or 24 h at a cell density of 1×10^6 cells/mL were added to porous hydroxyapatite (HA) disks of 5 mm in diameter (Apaceram, Pentax Corp., Tokyo, Japan) and incubated at 37°C for 3 h. The HA disks were transferred to 24-well Falcon tissue culture dishes and subcultured in media containing 15% FBS, 10 mM β-glycerophosphate, disodium salt, 0.07 mM L-ascorbic acid phosphate, and 0.1 μM Dex for 2 weeks for fabrication of MSCs/HA constructs. Seven-week-old male athymic nude Fischer 344 rats (Fischer 344/N Jcl-rnu, Clea Japan, Inc., Tokyo, Japan) were anesthetized by intramuscular injection of pentobarbital (Nembutal, Dainippon Pharmaceutical Co. Ltd., Osaka, Japan) at a final concentration of 3.5 mg/100 g body weight. Six MSCs/HA constructs and two HA disks without cells were implanted subcutaneously into the back of each athymic nude rat; three constructs fabricated from MSCs stored for 0 h and one HA disk without cells were implanted in the right side, and the other three constructs fabricated from MSCs stored for 24 h and one HA disk without cells were separately implanted in the left side. The recipient rats used were two. HA disks without cells were used as negative controls. Animal experiments were carried out in compliance with Japanese Law (No. 105) on animal protection and administration as well as the Regulation on the Imple-

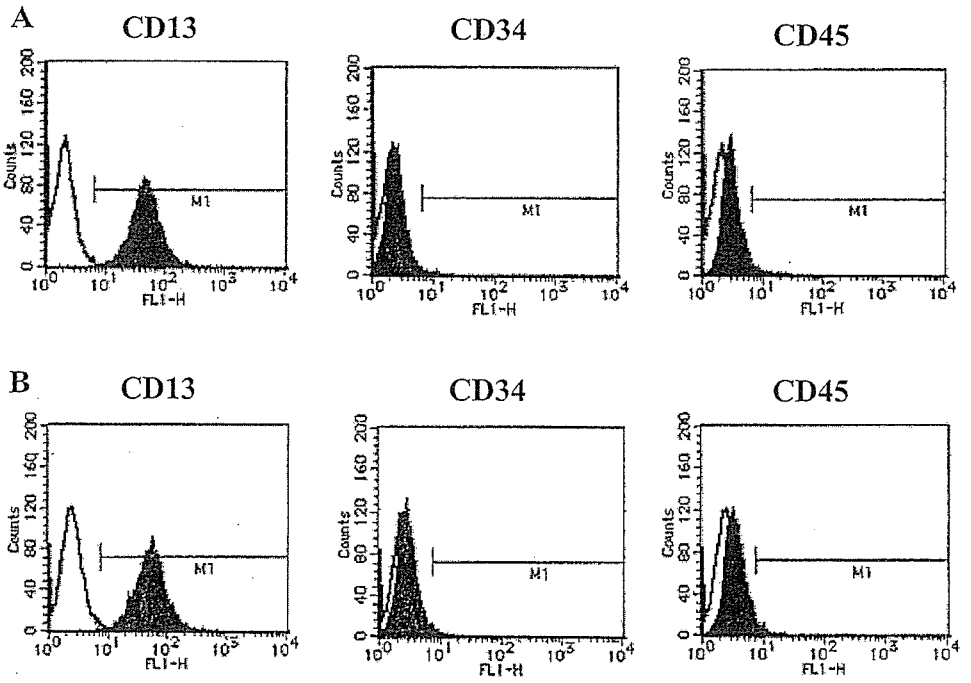

FIG. 3. FACS analysis of MSCs (**A**) and MSCs stored in PBS at 4°C for 24 h (**B**). Both cell types were reacted with each CD antibody and then loaded into a flow cytometer. The open histograms show the fluorescence intensity of the cells with negative control IgG. The closed histograms show the fluorescence intensity of the cells with each CD antibody.

mentation of Animal Experimentation of the AIST (Independent Administrative Organization, National Institute of Advanced Industrial Science and Technology).

Analysis of the implants

All implants (MSCs/HA constructs and HA disks without cells) were harvested 6 weeks postimplantation. Each of four constructs fabricated from MSCs stored for 0 h and 24 h, respectively, was used for ALP activity assay as described above. The other constructs and HA disks without cells were fixed with 10% buffered formalin, decalcified with K-CX solution (Falma Co., Tokyo, Japan), and then stained with hematoxylin and eosin. These specimens were examined by light microscopy.

Statistics

All the data were analyzed for statistical significance using Student's *t*-test computed by JMP 5.0 software (SAS Institute, Inc.), and statistical significance was accepted at $p < 0.05$. Experimental results were expressed as the means ± standard deviation (SD) of the mean.

RESULTS

Viability of MSCs suspended/stored in PBS

After culturing MSCs in 90-mm^2 tissue culture dishes for about 10 days, the cells were trypsinized and suspended with PBS at a concentration of 1×10^6 cells/mL and stored at 4°C, 24°C, and 37°C. The viability (percent of total cells that were viable) of the MSCs in the PBS was assayed by a NucleoCounter. The assay was done at different storage intervals (from 0 to 24 h). Cell viability was maintained at more than 80% at any temperature of 4°C, 24°C, and 37°C after 1 h, then gradually decreased over time. The decrease was most apparent for the MSCs stored at 37°C, showing about 61% viability after 24 h. At 4°C and 24°C after 6 h, viabilities were both about 85% and those after 24 h were about 81% and 70%, respectively (Fig. 1). Concerning the cells stored for 24 h, statistical differences are seen among the percent viabilities at 4°C, 24°C, and 37°C.

The viabilities at the single-cell level were visualized by a LIVE/DEAD Viability Assay Kit. As shown in Fig. 2, most cells were green (viable cells) and only a few

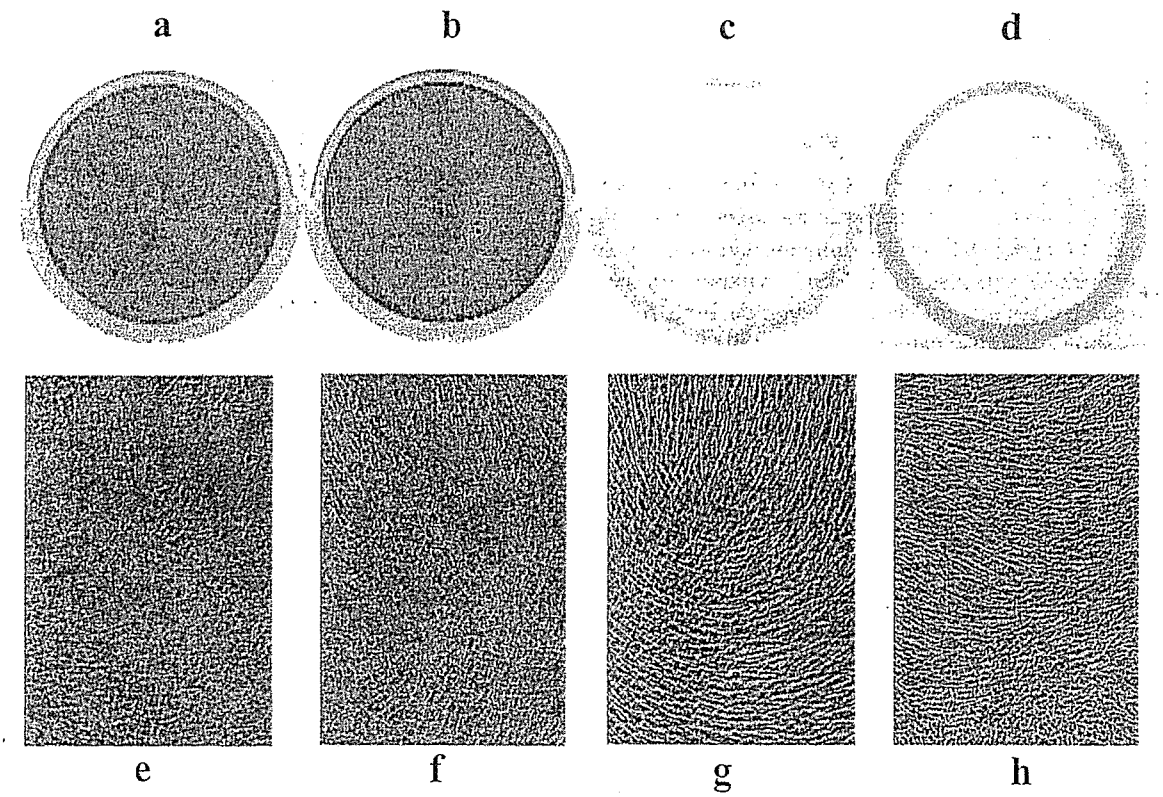

FIG. 4. Mineralization of MSCs on culture dishes. MSCs (**a, b, c, e, f,** and g) and human fibroblasts (d and h) were cultured in the presence of Dex (a, b, **d,** e, f, and **h**) or absence of Dex (c and g) for 21 days in 12-well plates. Culture medium contained glycerophosphate and calcium binding fluorescent dye of calcein. After being washed with PBS, the culture dish was visualized using an image analyzer. Fluorescence uptake (a, b, c, and d) and phase contrast view of culture (e, f, g, and h) are shown. MSCs stored in PBS at 4°C for 0 h (a and e) and 24 h (b, c, f, and g) were used for the culture. Black dots (a and b) indicate calcium deposition by fluorescence intensity. (Color images are available at <www.liebertpub.com/ten>.)

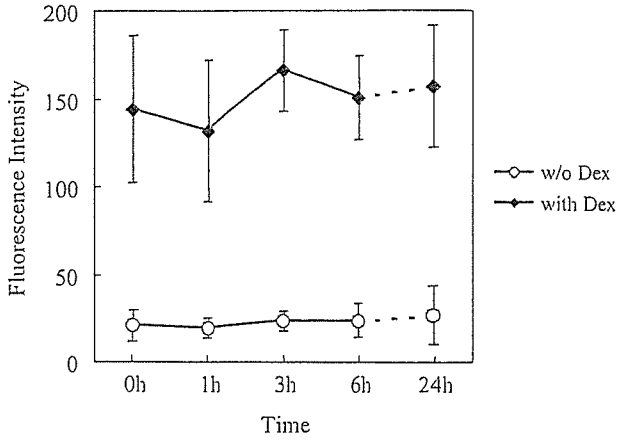

FIG. 5. Fluorescence intensity of cultured MSCs after being stored in PBS at 4°C from 0 h (immediately seeded) to 24 h. The culture occurred in the presence or absence of Dex for 14 days. The data represent the mean ± SD of the six samples.

cells were red (nonviable cells) in cultured MSCs before suspension in PBS. After the MSCs suspension/storage in PBS for 24 h at 4°C, 24°C, and 37°C, the number of green cells decreased, indicating a loss of viability. The percents of green cells (viable) at 4°C, 24°C, and 37°C were 82, 74, and 57, respectively. These data were comparable with those assayed by NucleoCounter (Fig. 1).

Immunostaining and FACS analysis

MSCs suspended/stored in PBS at 4°C after 24 h were analyzed by a flow cytometer for the expressions of CD13, CD34, and CD45 surface antigens and were compared with these expressions of MSCs without storage. Representative results are shown in Fig. 3. Both MSC samples showed similar patterns, that is, cells from both samples were not positive for the expression of hematopoietic markers of CD34 and 45, but strongly positive for CD13 (Aminopeptidase N), which is known to be present in MSCs.[25]

MSCs suspended/stored in PBS at 24°C and 37°C for 24 h also showed similar expression patterns (data are not shown). These results showed that the cell surface expression patterns had not been changed after being suspended/stored for 24 h. Only living cells were gated and analyzed.

Differentiation assay

MSCs suspended/stored in PBS at 4°C for 0 h (immediately used) to 24 h were seeded on a 12-well culture plate and cultured in osteogenic medium. The medium contained β-glycerophosphate, L-ascorbic acid 2-phosphate and, importantly, Dex, which is known to induce undifferentiated MSCs into osteoblasts,[8,21,22] resulting in the formation of a mineralized matrix. As we previously reported, the mineralization (bone matrix formation) could be detected after about 10 to 14 days of culture and more obviously after 21 days.[8,21] As shown in Fig. 4, the culture with Dex for 21 days showed mineralization (amorphous brown color in Fig. 4e and f), which was confirmed by calcein uptake (black areas in Fig. 4a and b). After storage in PBS, the mineralization capacity of MSCs (Fig. 4b and f) was comparable to that without storage (Fig. 4a and e). In contrast, the culture without Dex showed no mineralization (Fig. 4c and g).

Because fibroblasts never exhibit mineralization even culturing with Dex,[24] we also cultured human fibroblasts in the presence Dex as negative controls of differentiation assays. As shown in Fig. 4d and g, human fibroblasts stored at 4°C for 24 h before culture did not show mineralization. These qualitative results indicate that storage at 4°C for 24 h does not affect the osteoblastic differentiation capability of MSCs.

To demonstrate quantitative data, we measured the amount of mineralization and ALP activity, which localizes at the cell membranes of osteoblasts.[26] As shown in Fig. 5, the amounts of mineralization detected by fluorescent uptake of calcein were much higher for the culture in the presence of Dex compared with the culture in the absence of Dex. The high uptake was seen by culturing MSCs suspended/stored in PBS for 0 h to 24 h. The data coincided well with the data of ALP (Fig. 6), which also demonstrated the high ALP activity of MSCs cultured in the presence of Dex. The high level was also detected by culturing MSCs suspended/stored in PBS for 0 to 24 h. As shown in the results, MSCs maintained a high level of osteogenic ability *in vitro* after storage at 4°C for 24 h.

Next, we addressed the *in vivo* ability of MSCs after storage. We have previously reported that MSCs/HA con-

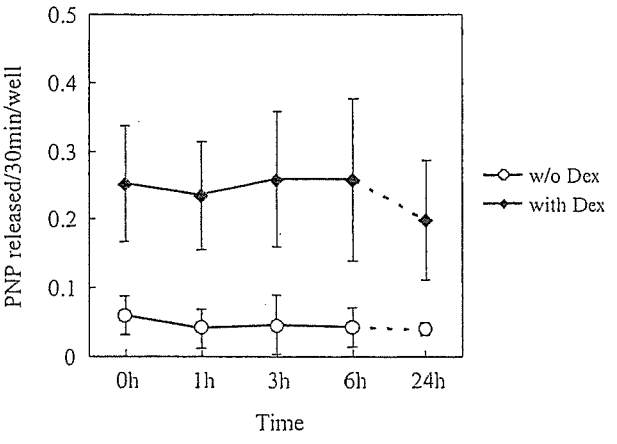

FIG. 6. ALP activity of cultured MSCs after being stored in PBS at 4°C from 0 h (immediately seeded) to 24 h. The culture occurred in the presence or absence of Dex for 14 days. The data represent the mean ± SD of the six samples (*p*-nitrophenol release/30 min/well).

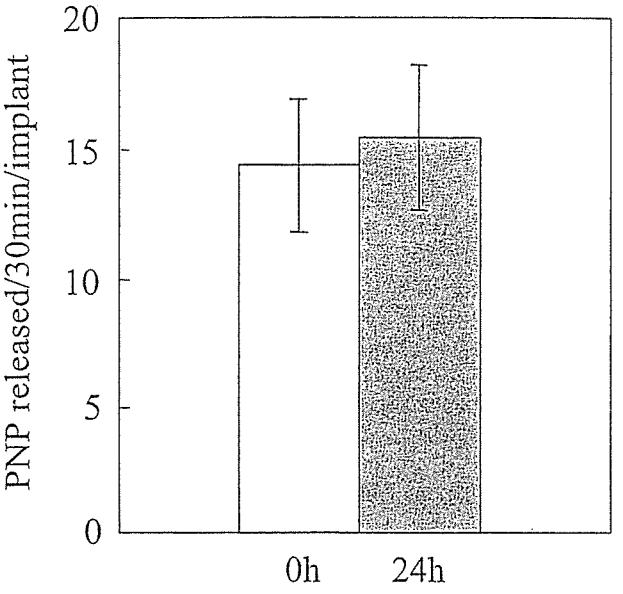

FIG. 7. ALP activity of MSCs/HA constructs after 6-week implantation. MSCs stored at 4°C for 0 h (open bar) or 24 h (closed bar) were cultured on HA disks with Dex for 2 weeks. The MSCs/HA constructs were implanted into athymic nude rats. After 6-week implantation, ALP activity of the constructs was measured. The data represent the mean ± SD of four samples (*p*-nitrophenol released/30 min/implant). (Color images are available at <www.liebertpub.com/ten>.)

structs treated with Dex could show a high level of osteogenic ability after *in vivo* implantation.[27] According to the methods, we prepared the constructs fabricated from MSCs stored at 4°C for 0 h or for 24 h and also HA disks without cells as negative controls, then implanted at subcutaneous sites of athymic nude rats. After 6-week implantation, both constructs showed similar high ALP activity (Fig. 7). Histologic appearance also demonstrated that both constructs showed newly formed bone with active osteoblasts (Fig. 8). However, implants of HA disks without cells did not show any bone formation (Fig. 8).

From these results, we concluded that MSCs suspended/stored in PBS at 4°C up to 24 h could maintain a high level of viability and capability of differentiation *in vitro* as well as *in vivo*.

DISCUSSION

Mesenchymal stem cells (MSCs) can differentiate into osteogenic lineage, and the osteogenic potential of MSCs has already been applied in clinical situations.[6,7,14] Recent studies have also demonstrated the possibility that MSCs can differentiate into other types of tissue-specific cells such as cardiac myoblasts,[15,16] vascular endothelial cells,[17,18] hepatocytes,[19] and neural cells.[20] These results indicate the usefulness of multipotential MSCs for a wide range of tissue engineering purposes in regenerative medicine. In considering the clinical applications of MSCs, the number of MSCs in bone marrow is extremely low,[2,13] and thus a procedure for culture expansion of MSCs is needed. However, such procedures introduce risks for bacterial/fungal contamination. To avoid these risks, biologically safe areas such as a cell processing center (CPC) having clean rooms and careful/safe handling are required. However, it is difficult to provide these facilities in many hospitals, primarily because of limited finances. Therefore, there has been an attempt to establish CPCs, which are available upon request by hospitals. This situation requires delivery of the cultured MSCs from the CPC to the hospital in need. The MSCs must be stored in optimal conditions that guarantee their viability as well as differentiation capability for a specific period.

When hematopoietic cells are stored in suspension, a temperature of around 4°C is recommended to maintain cell viability and function.[28] However, there is no simi-

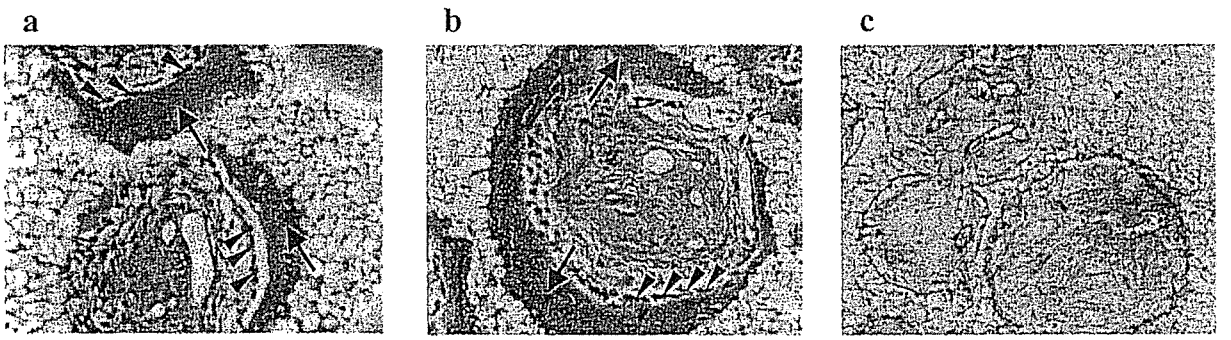

FIG. 8. Histological appearance of MSCs/HA constructs after 6-week implantation. MSCs stored at 4°C for 0 h (a) or 24 h (b) were cultured on HA disks with Dex for 2 weeks. The MSCs/HA constructs were implanted into athymic nude rats. After 6-week implantation, the constructs were decalcified and stained with hematoxylin and eosin. HA disks without MSCs were implanted as negative controls (c). The light microscopy was performed. Arrows show bone matrices in porous areas of HA. Arrowheads show the bone forming active osteoblasts. Original magnification ×200.

lar information about the optimal temperature and conditions for maintaining the viability of adherent cell MSCs. This study focused on investigating viability assessment for successful transportation of MSCs in suspension based on three major factors: incubation time, type of storage medium, and temperature. We also examined osteogenic differentiation capability of MSCs stored in suspension.

Our preliminary data showed that there was no difference of MSC viability in the three kinds of media, PBS, saline, and α-MEM (data not shown). Among them, the composition of PBS and saline are simpler than that of α-MEM. Saline may cause pH changes because there is no buffering action. For these reasons, in the present study we selected PBS as the storage medium for MSCs.

As shown in Fig. 1, MSCs maintained more than 85% viability at both 4°C and 24°C for 6 h, and more than 80% viability at 4°C for 24 h, whereas the viability of the cells stored at 24°C and 37°C for 24 h was significantly decreased. Because the viability at 4°C was most acceptable and it is relatively easy to regulate/maintain the temperature at 4°C, we further performed osteogenic differentiation assay *in vitro* as well as *in vivo* using the cell stored at 4°C. The MSCs suspended/stored in PBS at 4°C for 24 h did not lose their capability for *in vitro* osteogenic differentiation. This is confirmed by the high degree of mineralization and ALP activity of the MSCs after culturing in the presence of Dex (Figs. 4–6). Importantly, the mineralization and ALP activities were comparable to those of control MSCs (nonstored MSCs). The expression of cell surface antigen patterns was similar for the MSCs stored for 24 h and the control MSCs. Consistent with the *in vitro* findings, *in vivo* implants of MSCs/HA construct demonstrated high ALP activity and bone-forming capability using MSCs after the storage. These results thus demonstrated that MSCs can maintain cell viability and osteogenic capability even after 24 h when stored in PBS at 4°C. These conditions enable the delivery of MSCs to distant medical facilities without serious loss of MSC function for the various purposes of tissue regeneration, especially hard tissue regeneration.

The present data clearly showed the durability of MSCs suspended/stored in PBS and that MSCs can be available not only locally but also in distant areas without significant loss of viability as well as differentiation (especially osteogenic differentiation) capability. Therefore, this process represents an opportunity for developing new therapeutic strategies using MSCs.

ACKNOWLEDGMENTS

We thank our colleagues at the National Institute of Advanced Industrial Science and Technology (AIST) and at Nara Medical University. This work was supported by the Three-Dimensional Tissue Module Project of METI (a Millennium Project) and a Grant-in-Aid for Scientific Research.

REFERENCES

1. Owen, M. Marrow stromal stem cells. J. Cell. Sci. Suppl. **10,** 63, 1988.
2. Caplan, A.I. Mesenchymal stem cells. J. Orthop. Res. **9,** 641, 1991.
3. Pittenger, M.F., Mackay, A.M., Beck, S.C., Jaiswal, R.K., Douglas, R., Mosca, J.D., Moorman, M.A., Simonetti, D.W., Craig, S., and Marshak, D.R. Multilineage potential of adult human mesenchymal stem cells. Science **284,** 143, 1999.
4. Ohgushi, H., and Okumura, M. Osteogenic capacity of rat and human marrow cells in porous ceramics. Acta Orthop. Scand. **61,** 431, 1990.
5. Caplan, A.I., and Bruder, S.P. Mesenchymal stem cells: Building blocks for molecular medicine in the 21st century. Trends Mol. Med. **259,** 7, 2001.
6. Horwitz, E.M., Gordon, P.L., Koo, W.K., Marx, J.C., Neel, M.D., McNall, R.Y., Muul, L., and Hofmann, T. Isolated allogeneic bone marrow-derived mesenchymal cells engraft and stimulate growth in children with osteogenesis imperfecta: Implications for cell therapy of bone. Proc. Natl. Acad. Sci. U S A **99,** 8932, 2002.
7. Quarto, R., Mastrogiacomo, M., Cancedda, R., Kutepov, S. M., Mukhachev, V., Lavroukov, A., Kon, E., and Marcacci, M. Repair of large bone defects with the use of autologous bone marrow stromal cells. N. Engl. J. Med. **344,** 385, 2001.
8. Maniatopoulos, C., Sodek, J., and Melcher, A.H. Bone formation *in vitro* by stromal cells obtained from bone marrow of young adult rat. Cell Tissue Res. **254,** 317, 1988.
9. Ohgushi, H., Dohi, Y., Katuda, T., Tamai, S., Tabata, S., and Suwa, Y. *In vitro* bone formation by rat marrow cell culture. J. Biomed. Mater. Res. **32,** 333, 1996.
10. Bruder, S.P., Jaiswal, N., and Haynesworth, S.E. Growth kinetics, self-renewal, and the osteogenic potential of purified human mesenchymal stem cells during extensive subcultivation and following cryopreservation. J. Cell Biochem. **64,** 278, 1997.
11. Ohgushi, H., Yoshikawa, T., Nakajima, H., Tamai, S., Dohi, Y., and Okunaga, K. Al_2O_3 doped apatite-wollastonite containing glass ceramic provokes osteogenic differentiation of marrow stromal stem cells. J. Biomed. Mater. Res. **44,** 381, 1999.
12. Kitamura, S., Ohgushi, H., Hirose, M., Funaoka, H., Takakura, Y., and Ito, H. Osteogenic differentiation of human bone marrow-derived mesenchymal cells cultured on alumina ceramics. Artif. Organs **28,** 72, 2004.
13. Ohgushi, H., and Caplan, A.I. Stem cell technology and bioceramics: From cell to gene engineering. J. Biomed. Mater. Res. **48,** 913, 1999.
14. Ohgushi, H., Kotobuki, N., Funaoka, H., Machida, H., Hirose, M., Tanaka, Y., and Takakura, Y. Tissue engineered ceramic artificial joint: *Ex vivo* osteogenic differentiation of patient mesenchymal cells on total ankle joints for treatment of osteoarthritis. Biomaterials **26,** 4654, 2005.